BSGF - Earth Sciences Bulletin 2021, 192, 41
© E. Vennin *et al.*, Published by EDP Sciences 2021
https://doi.org/10.1051/bsgf/2021030

BSGF Earth Sciences Bulletin
Available online at:
www.bsgf.fr

The Limagne Basin: a journey through modern and fossil microbial deposits☆

Emmanuelle Vennin[1,*], Anthony Bouton[1,2], Adeline Roche[1], Emmanuelle Gérard[3], Irina Bundeleva[1], Pierre Boussagol[1], Aurélia Wattinne[4], Christophe Kolodka[5], Eric Gaucher[5], Aurélien Virgone[5] and Pieter T. Visscher[1,2]

[1] Biogéosciences, UMR 6282 CNRS, Université Bourgogne Franche-Comté, 6 Boulevard Gabriel, 21000 Dijon, France
[2] University of Connecticut, Departments of Marine Sciences & Geosciences, Groton, CT 06340/CT 06269, USA
[3] Institut de Physique du Globe de Paris, UMR 7154 CNRS, 75005 Paris, France
[4] Rue Charles Ladreit de la Charrière, 5, 78870 Bailly, France
[5] Total CSTJF, Avenue Larribau, F-64018 Pau Cedex, France

Received: 5 October 2020 / Accepted: 24 August 2021 / Publishing online: 18 October 2021

Abstract – The Limagne Basin (Massif Central, France) originated during a major, European-scale, extensive event (European Cenozoic Rift System), which led to the formation of several rift systems in the foreland of the Alps between the Upper Eocene and Pliocene. A fluvio-lacustrine system emplaced in the basin and resulted in a mixed carbonate-siliciclastic sedimentation in which microbial and metazoan buildups occupy an important place. However, microbial deposits are not exclusive to the Cenozoic history of the Limagne Basin; nowadays, in the basin, they still form in association with thermal spring systems. A fieldtrip was carried out in the Limagne Basin as part of the *Microbialites: formation, evolution and diagenesis (M-Fed)* meeting (October 2019). The objective of this excursion was to assess the diversity of modern and fossil (Chattian to Aquitanian) microbial sediments and structures in three prime locations (the Jussat and Chadrat outcrops and the Grand Gandaillat quarry). A detailed description of the morphologies and fabrics of the buildups and their associated biotic components can be used to discuss the spatio-temporal distribution pattern. Different basin margin models are proposed based on the changes in the distribution, morphology and size of the microbial and metazoan-rich deposits through time. The Jussat outcrop offers novel perspectives to unravel the evolution of the lacustrine/palustrine cycles over time and to establish a long-term paleoenvironmental history of the western margin of the basin during the Aquitanian. These cycles are composed of (i) lacustrine sedimentation comprising microbial and metazoan buildups and organic matter-rich marls reflecting a period of high accommodation, and (ii) palustrine deposits made of mudstones and clayey paleosoils, indicative of a period of low accommodation. It is suggested that climatic, tectonic, volcanic and local parameters (physiography, substrate) control the deposition of the buildups in each of the different cycles. In addition, the modern microbial mats of the Sainte-Marguerite and La Poix outcrops offer an opportunity to constrain the controlling processes at the origin of the mineralization involved in the formation of the microbialites and their preservation in the fossil record.

Keywords: Limagne / Massif Central / fossil and modern microbialites / Oligocene-Miocene / fieldtrip / carbonates

Résumé – Le bassin des Limagnes : une excursion à travers les dépôts microbiens modernes et fossiles. Le bassin des Limagnes (Massif Central) est issu de la mise en place d'une phase de rifting liée à la géodynamique Ouest-Eropéenne (Rift Ouest Européen) entre l'Eocène Supérieur et le Pliocène. Il représente un lieu privilégier pour étudier les bioconstructions à microbialites et métazoaires qui s'inscrivent dans une sédimentation mixte carbonate-terrigène fluvio-lacustre. Ce secteur bénéficie par ailleurs de la présence de tapis microbiens modernes. L'excursion organisée en octobre 2019, à l'occasion du colloque

☆ This manuscript results from a fieldtrip organized as part of the "*M-Fed Microbialites: formation, evolution, diagenesis*" meeting held in Dijon, on October 26–27th, 2019 [Cet article est écrit suite à une excursion en Limagne lors du congrès « *M-Fed Microbialites: formation, evolution, diagenesis* » organisée les 26–27 octobre 2019].

*Corresponding author: emmanuelle.vennin@u-bourgogne.fr

Microbialites: formation, evolution and diagenesis, dans cette région permet d'observer et d'approcher la diversité et la structuration de sédiments microbiens modernes et fossiles. Une description détaillée de la morphologie, des fabriques des bioconstructions chattiennes et aquitaniennes et de leurs composants biotiques, des affleurements de Jussat et Chadrat et dans la carrière de Grand Gandaillat, fournit un éclairage concernant leur organisation spatio-temporelle. Les changements de distribution, de morphologie et de taille des bioconstructions à microbialites et métazoaires à travers le temps permettent de proposer plusieurs modèles de rampe lacustre. Les cycles palustre/lacustre ont fait l'objet de publication récente, toutefois le site de Jussat offre des conditions d'affleurement exceptionnelles qui soulignent le rôle du climat et de la tectonique dans la mise en place de cette cyclicité. Ces cycles sont organisés en une succession de dépôts : (1) lacustres composés de bioconstructions à microbialites et métazoaires et de marnes riches en matière organique qui indiquent des périodes de forte accommodation et (2) de dépôts palustres boueux et argileux à paléosols soulignant des périodes de faible accommodation. Le climat, la tectonique, le volcanisme mais également des paramètres locaux tels que la physiographie des lacs et le substrat sont impliqués dans la formation des bioconstructions et leur organisation au sein des différents cycles sédimentaires. De plus, les tapis microbiens modernes de Sainte-Marguerite et de La Poix viennent offrir une opportunité de comprendre les processus de minéralisation à l'origine de la formation des microbialites et de leur préservation dans le registre fossile.

Mots clés : Limagne / Massif Central / microbialites fossiles et modernes / Oligocène-Miocène / excursion / carbonates

1 Introduction

The accumulation and preservation of lacustrine microbial carbonates in both recent systems (*e.g.* Lake Tanganyika, Kenya; Casanova and Hillaire-Marcel, 1992; Cohen *et al.*, 1997; Great Salt Lake, USA, *e.g.* Carozzi, 1962; Bouton *et al.*, 2016; Vanden Berg, 2019; Vennin *et al.*, 2019) and ancient systems (*e.g.* Green River Formation, USA; Seard *et al.*, 2013; Chidsey *et al.*, 2015) have been the focus of numerous studies with the aim to better constrain their petrology and isotopic composition with regards to the sedimentary and geodynamic context and to ultimately understand the processes leading to their formation. Microbial deposits have been at the center of interest of many studies since the discovery of extensive examples of these associated with petroleum reservoirs and, in particular, because of the rush to find the best modern and/or fossil analogues (*e.g.* Paik, 2005; Seard *et al.*, 2013; He *et al.*, 2015; Chidsey *et al.*, 2015; Gong *et al.*, 2017; Adiya *et al.*, 2017; Roche *et al.*, 2018). Lacustrine microbialites have been linked to economically significant petroleum systems, especially prolific in the Lower Cretaceous "pre-salt" systems found offshore Brazil and Angola (Awramik and Buchheim, 2012; Wasson *et al.*, 2012; Mello *et al.*, 2013; Muniz and Bosence, 2015; Gomes *et al.*, 2020) and the Eocene Green River Formation within the Uinta Basin in Utah, USA (Bradley, 1924; Loewen *et al.*, 1999; Leggitt and Cushman, 2001; Leggitt *et al.*, 2007; Seard *et al.*, 2013; Chidsey *et al.*, 2015; Hurst *et al.*, 2018). The Limagne Basin, located in the French Massif Central, shares numerous geodynamical (*e.g.*, a normal fault system framework linked to a rifting system and volcanic activity; Davison, 2007) and sedimentological (diverse and abundant lacustrine microbialites; Bertrand-Sarfati *et al.*, 1966; Donsimoni and Giot, 1977; Freytet, 2000; Wattinne *et al.*, 2003; Roche *et al.*, 2018) characteristics with the South-Atlantic "pre-salt" basins and therefore represents an exceptional analogue.

The Limagne Basin originated from a rifting phase linked to a major, continental-scale, extensive geodynamic event (European Cenozoic Rift System) affecting the foreland of the Alps between the Upper Eocene and Pliocene. It represents an unsurpassed location to investigate the sedimentary dynamics of microbial and metazoan buildups deposited as part of a fluvio-lacustrine mixed carbonate-siliciclastic sedimentary system during the Oligocene and Miocene. Additionally, is that extensive microbial mats still currently form associated with the thermal activity of the region, which in turn is directly linked to the tertiary geodynamic framework? Despite showing great similarities with the world-famous Eocene buildups of the Green River Formation (*e.g.* morphologies, composition, distribution, associated sedimentation and presence of hydrocarbons), the buildups of the Limagne Basin have attracted less interest, even though their existence has been reported for a long time (D'Halloy, 1812). Most of the previous studies were limited to a detailed description of the morphology and composition of these buildups and fail to include the spatial and temporal evolution or the paleo-environmental significance of these deposits. After characterizing the various microbial buildups, and reconstructing the associated paleo-environments, Wattinne *et al.* (2003) and Wattinne (2004) suggested that the morphologies and distribution of the bioconstructions were mostly controlled by the organisms (microbes *vs.* metazoans) involved in the buildups, the available space and the fluctuations of the shorelines. However, this work was mainly concentrated in the northern part of the Limagne Basin. Based on the detailed investigations carried out on microbial and metazoan buildups preserved in the southern and central Limagne basins, Roche *et al.* (2018) showed that the sedimentary cycles were mostly driven by a superimposition of regional (climatic, tectono-volcanism) and local factors, controlling the chemical and physical changes of the waterbody, the vegetation covers and the physiography of the lake margin. Over a large scale, climate and tectonics directly affect the morphology of lakes and their watersheds and then are considered as first-order factors controlling sedimentation. When coupled, these two major factors may strongly and quickly impact base level variations and therefore accommodation in lacustrine environments (Bohacs *et al.*, 2013). The hydrology of the lake is also

a determining factor in the onset of sedimentation and intense carbonate precipitation (Owen and Crossley, 1992). Although often neglected, dissolved solids produced by weathering processes contribute significantly to the sedimentary dynamics of basins, supporting chemical and/or biological precipitation. Dissolved solids are delivered to the basin by surface flow through local rivers and also from subsurface flow through faults. The chemistry of the lake mostly results from the balance between the inputs and outputs of dissolved solids and the precipitation/evaporation ratio (Bouton *et al.*, 2019). The precipitation of solid matter from the dissolved load of the lakes occurs either abiotically (driven by inorganic thermodynamics and reaction kinetics) or biotically (as a consequence of metabolism). Inorganic and/or organic mediated carbonate precipitation processes occur in lacustrine settings as a function of water chemistry, carbonate supersaturation, skeletal biota, vegetation, algae and microorganisms (Pedley, 1990, 2014; Riding, 2008, 2011; Pentecost, 2005; Dupraz *et al.*, 2009; Della Porta, 2015). As proposed by Ginsburg (1991), the environment shapes the morphology, but the microorganisms involved determine the microstructures. In the fossil record, it remains difficult to disentangle the role of both biotic and abiotic processes as they are closely coupled and carbonate precipitation results from a balance between both processes.

In this manuscript, we focus on the diversity of modern and fossil (Oligo-Miocene) microbial sediments and structures emplaced in the Limagne Basin. As part of the two-day excursion organized during the 2019 M-Fed meeting, the focus was on the central part of the basin, while observations from the northern and southern parts will be summarized from the literature. Based on the analysis of the different outcrops and/or quarries, we will discuss: (1) the geometry and composition of the microbial-rich deposits and their association with other biotic components (algae, insects, mollusks); (2) the main depositional environments of the lacustrine sediments in the central Limagne Basin; (3) the factors controlling the development of microbial and metazoan-rich buildups as well as their spatial and temporal evolution; and finally, (4) the mineralization processes associated with the formation of buildups and microbial mats through a modern system.

2 Geological context

The Limagne Basin corresponds to a north-south oriented half-graben, the largest of the Massif Central Rift (35 km large, Fig. 1A). This basin formed during the Tertiary (Bergerat, 1987) and belongs to the European Cenozoic Rift System (Merle *et al.*, 1998; Michon and Merle, 2001; Sissingh 2001; Dèzes *et al.*, 2004). The basin is divided into the "Limagne Bourbonnaise" in the north, the "Limagne de Clermont" in the central part and the "Limagne d'Issoire" in the south (Fig. 1B). The Limagne half-graben is bounded to the west by a major north-south normal fault: the Limagne fault (Figs. 1B and 2; Michon, 2000). This basin is subdivided by secondary transverse strike-slip faults (*i.e.* the Aigueperse fault; Fig. 1B), responsible for the formation of several sub-basins of varying sizes, such as the Moulins, Vichy, Riom, Lembron and Brioude grabens (Donsimoni, 1975; Riveline *et al.*, 1988; Merle *et al.*, 1998; Sissingh, 2001). Due to its half-graben architecture (Fig. 1C), the Limagne Basin is asymmetric with a thick sedimentary succession (reaching 2500 m) in the western part, in the Riom Trough, while thinner deposits are recorded in the eastern part (Grolier and Tchimichkian, 1963; Morange *et al.*, 1971; Pelletier, 1972). During the last 45 years, several geophysical and structural geologic studies on the deep structure of the crust and upper mantle of the Massif Central and the Chaîne des Puys have been undertaken. Following Perrier and Ruegg (1973), who revealed thinning in the Limagne Basin, the ECORS profiles (Sobolev *et al.*, 1997; Zeyen *et al.*, 1997) have shown that the warm mantle components beneath the Auvergne volcanoes have risen from a depth of at least 250 km. Merle and Michon (2001) and Dèzes *et al.* (2004) proposed a two-stage model: lithospheric thinning caused by alpine Eocene-Oligocene subduction (passive tearing), followed by thermal erosion (Miocene higher-current) of the Alps (active rifting).

The filling of the Limagne Basin extends from the lower Eocene to the lower Miocene. It is characterized by five sedimentary cycles delimited by erosional surfaces for which the amplitude and intensity vary from the margins to the center of the basin (Genter *et al.*, 2003). Each of these cycles begins with the deposition of detrital sediments (conglomerates and sandstones), which then transition to marls and/or limestones before ending with evaporitic deposits or carbonate buildups.

As part of the fieldtrip, special attention was paid to the Oligocene-Miocene deposits (Chattian to Aquitanian) of the central Limagne Basin. The Oligo-Miocene lacustrine buildups contain prokaryotes (microbes) as well as the discussed eukaryotic algae (*Cladophorites*) or metazoans (mainly insects, especially caddisflies, and mollusks). Caddisfly larvae (Trichoptera) live in aquatic environments and make a protective (pupal) case that can be stacked in clusters (Mackay and Wiggins, 1979; Hugueney *et al.*, 1990). The distribution of the buildups is non-random and is determined by the dynamics of the shoreline, as well as to the tectonic framework as they are distributed along fault corridors (Fig. 2; Wattinne *et al.*, 2003; Roche *et al.*, 2018).

During the Chattian, the salinity of the lake decreased as deduced from the absence of evaporitic sediments (Wattinne *et al.*, 2018). A (weak) volcanic activity was recorded during this period which was manifested by injections of magma into wet and non-indurated sediments, resulting in the formation of volcaniclastic, phreatomagmatic rocks called "peperites" (Skilling *et al.*, 2002; site of Grand Gandaillat). The Upper Chattian was characterized by the deposition of marls and concreted ("concretionned" sensu Dangeard, 1931) limestones in freshwater lacustrine environments (Bertrand-Sarfati *et al.*, 1966; Rey, 1971; Donsimoni, 1975; Gorin, 1975; Donsimoni and Giot, 1977; Sissingh, 2001), recording a widespread cooling and arid climatic episode (Gorin, 1975; Giot *et al.*, 1976; Hugueney, 1984).

The lacustrine environments associated with weak volcanic activity (with the deposition of "peperites") recorded during the Chattian persisted during the Miocene. During the Aquitanian, warm and relatively wet conditions supported the formation of concreted limestones (Chateauneuf, 1972; Hugueney, 1984; Utescher *et al.*, 2000; Wattinne *et al.*, 2003; Scherler *et al.*, 2013). During the remainder of the Miocene, the sedimentation, which was still lacustrine, became more detrital and consisted of siliciclastic sands called "Bourbonnais sands" (Rey, 1971; Donsimoni, 1975;

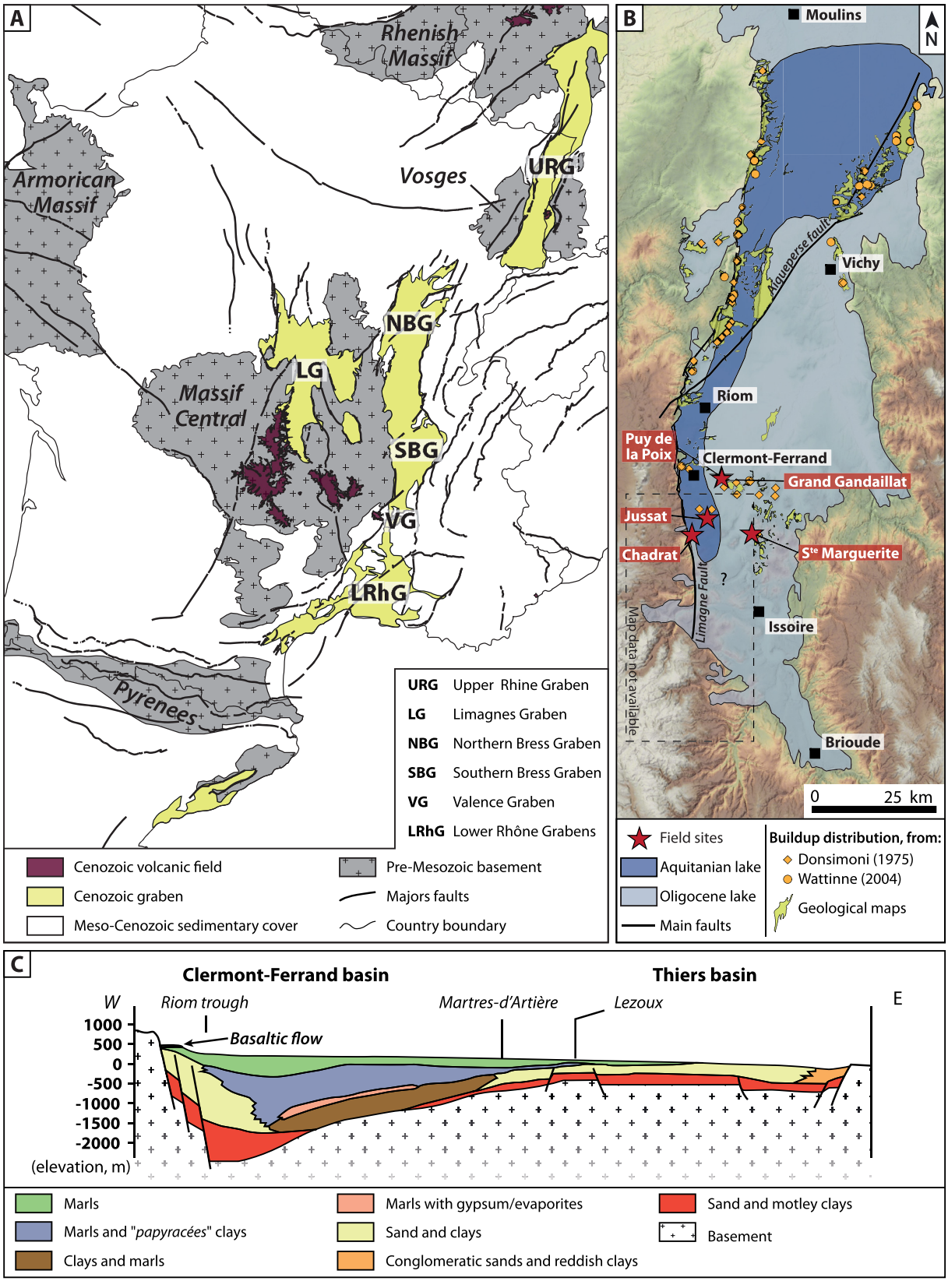

Fig. 1. A. Structural map of the western part of the European Cenozoic Rift System, a succession of (half)grabens extending from the Mediterranean Sea to the Bohemian and Rhenish Massifs (after Dèzes *et al.*, 2004 and BRGM, 2006). B. Map of the Limagne Basin showing the main study site and their relation with the paleogeographic extensions of the lake during the Oligocene and Miocene (adapted from Hugueney *et al.*, 1999) and distribution of the buildups. The base map corresponds to the Digital Elevation Model over Europe from the GMES RDA project (EU-DEM). C. Geological E-W transect of the Central Limagne (after Morange *et al.*, 1971; Wattinne, 2004).

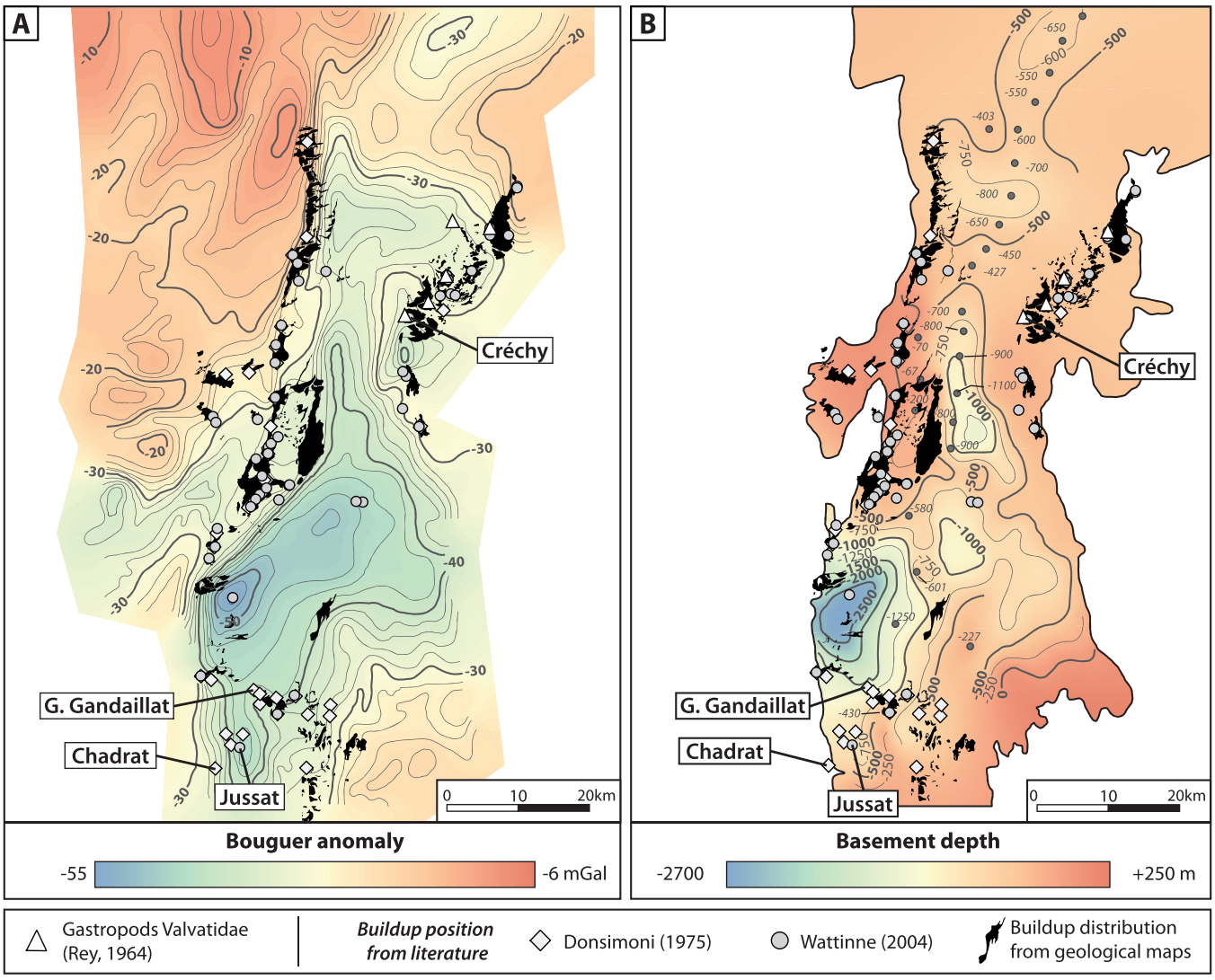

Fig. 2. (A) Gravity (Bouguer) anomaly (in mGal) and (B) basement depth (in m below/above sea level) maps of the Limagne Basin (after Morange *et al.*, 1971). Contour lines and point data from Morange *et al.* (1971) maps were interpolated into a raster map using ArcMap ("Topo to Raster" tool, applying ANUDEM (Australian National University Digital Elevation Model) program; Hutchinson, 1988, 1989) producing continuous data. The distribution of microbial and/or metazoans buildups and Valvatidae gastropods is based on literature data.

Donsimoni and Giot, 1977; Hugueney *et al.*, 1990, 1999, 2003; Sissingh, 2001; Wattinne *et al.*, 2003).

The maximum extension of the lake was reached during the Oligocene where the three Limagne sub-basins were flooded (100's kilometers; Hugueney *et al.*, 1999). During the early Miocene, a volcano-tectonic uplift was responsible for the lowering of the subsidence rate (Sissingh, 2001; Dèzes *et al.*, 2004) resulting in the northward migration of the depocenter toward the Limagne Bourbonnaise Basin; the central and southern parts of the basin (the central Limagne Basin) only consisted of a narrow channel along the western Limagne main fault (Hugueney *et al.*, 1999). The lacustrine domain remained confined to the northern part of the Limagne Bourbonnaise Basin during the upper Aquitanian (Fig. 1B), before disappearing completely in the Burdigalian and giving way to a fluvial system (Wattinne *et al.*, 2003).

3 Location and description of the outcrops

Five outcrops were visited during the fieldtrip organized in the Limagne Basin during the 2019 M-Fed meeting: (i) Chadrat, (ii) Jussat, (iii) Grand Gandaillat, (iv) Puy de la Poix and (v) Sainte-Marguerite.

(i) The Chadrat outcrop (commune of Saint-Saturnin; 45°40'06.51"N, 003°05'15.85"E) is located 12 km to the south of Clermont-Ferrand, along the Montagne de la Serre (Figs. 3A and 3B). This outcrop is rich in carbonate buildups, commonly called "stromatolites". They were used as building material for numerous houses in the villages of Chadrat and Saint-Saturnin. This outcrop is maintained and protected by the Arkose Association (https://arkose-chadrat.pagesperso-orange.fr) to increase the value of the heritage sites located in Chadrat. The carbonate buildups form a continuous layer up to 5 m

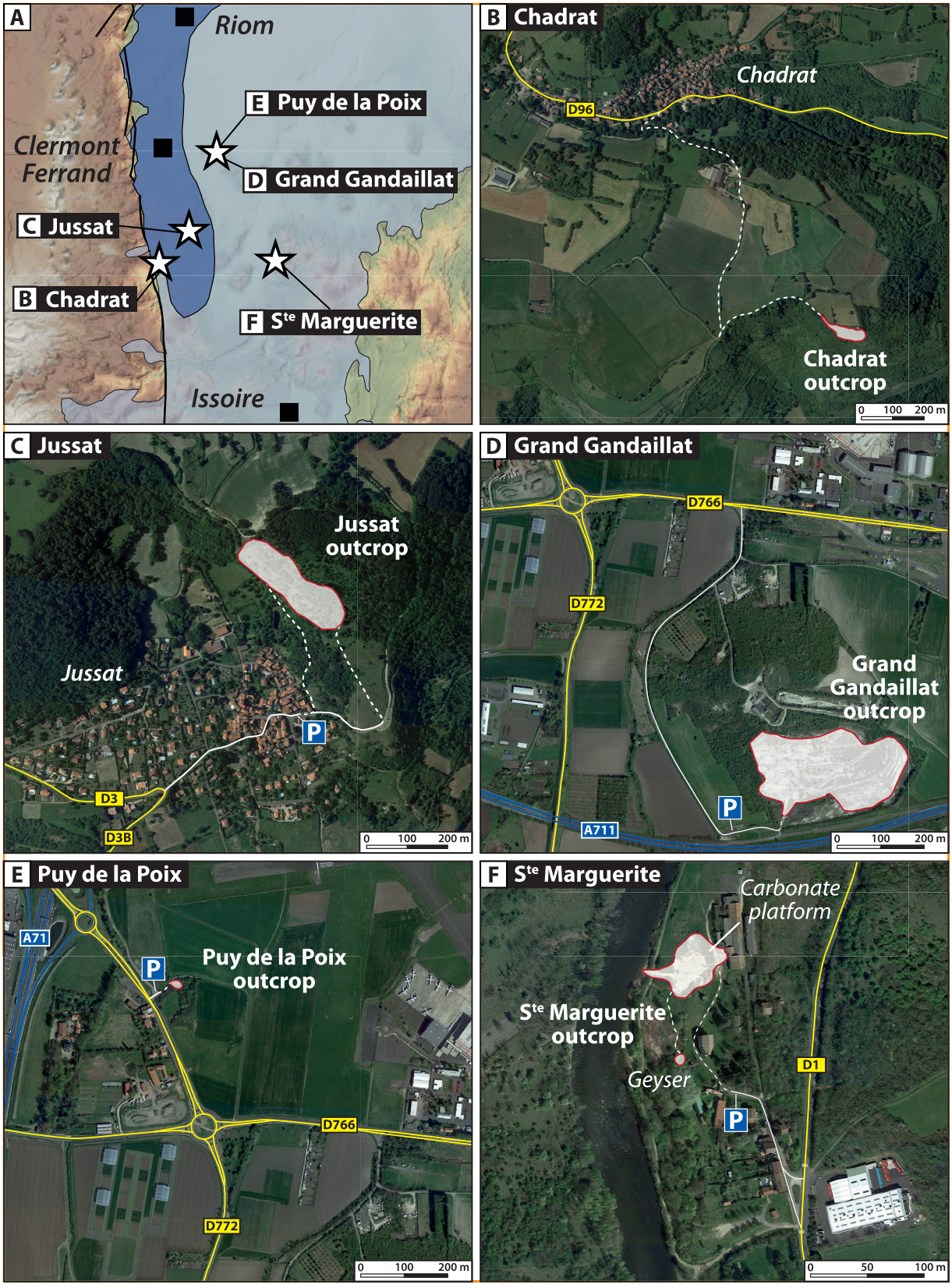

Fig. 3. A. Map showing the paleogeographic extensions of the lake during the Oligocene and Miocene (adapted from Hugueney *et al.*, 1999) of the Limagne Basin and localization of the visited sites during the m-fed fieldtrip (satellite images from © Microsoft Corporation – Imagery © Harris Corp, Earthstar Geographics LLC). B. Localization of the Chadrat outcrop. C. Jussat outcrop (ancient quarry). D. Grand Gandaillat quarry. E. Puy de la Poix outcrop. F. Saint Marguerite outcrop with the modern carbonate platform.

thick, with an unique biostromal morphology at the scale of the Limagne Basin (Figs. 4A, 5 and 6). They consist of planar, globular and hemispherical structures (Donsimoni, 1975). These buildups comprise molds of microbial filaments that are included in micritic to sparitic matrices and which are described by Freytet (1998, 2000) as being different species of algae associated with bacteria. Although estimated as Oligo-Miocene in age, no precise ages have been defined in the literature for these carbonate deposits. However, a similar sedimentary succession has been observed capping the Jussat deposits.

(ii) The Jussat outcrop (45°42'13.29"N, 3°6'30.93"E) belongs to the commune of Chanonat. It is located approximately 8 km south of Clermont-Ferrand and 4 km north of the Chadrat outcrop (Figs. 3A, 3C, 4B, 5 and 7). The Jussat outcrop constitutes a prime, albeit poorly described, outcrop for investigating the lacustrine sedimentation of the Limagne Basin. This outcrop, roughly 55 m high, is an old quarry that is now abandoned and can be freely accessed. No precise dating has been carried out for the deposits in this quarry. Donsimoni (1975) placed these deposits at the Oligocene-Miocene boundary, while Freytet (2000) and the geological map of Clermont-Ferrand (1:80 000 scale) indicated an Oligocene age (Rupelian and Lower Chattian). A nearby outcrop, La Roche-Blanche, 2 km east of Jussat and at almost the same altitude, is dated based on the analysis of mammal fossils as early Miocene (Hugueney *et al.*, 1999).

(iii) The Grand Gandaillat quarry is located in the town of Clermont-Ferrand (45°46'20.34"N, 3°9'15.10"E; Figs. 3A, 3D, 4C, 5 and 8). It is part of the Cournon-Lempdes Plateau, which is estimated to date back to the late Oligocene, based on mammalian and malacological biozones (Rey, 1971; Aubert *et al.*, 1973). Between 1985 and 1987, the company Forezienne extracted approximately one million m^3 of marl-limestone for the construction of the Clermont-Ferrand A71 highway. This quarry was almost completely filled in and served a rest area for a service station. In 2014, under pressure from numerous geologists, it was taken over by the town of Clermont-Ferrand. Since then, it has been managed by the Auvergne Conservatory of Natural Spaces and it is signposted for visitors. For security reasons, the quarry is closed to the public but can be visited upon request at the Clermont-Ferrand town hall (*mairie*). Each year, this geosite is visited by more than 6000 middle school students and high school students (www.puy-de-dome.gouv.fr). Located in the Limagne half-graben, on the western edge of the Cournon horst (Michon, 2000), this quarry provides access to a sedimentary series that is roughly thirty meters thick and visible on several successive fronts (Roche *et al.*, 2018). Although it is difficult to precisely date, the estimated age of these deposits is late Oligocene (Chattian, Rey, 1971). The sedimentary succession is impacted by numerous faults, reflecting both the Oligocene extension and the post-Oligocene uplift of the basin (Michon, 2000).

(iv) The Puy de la Poix (altitude 345 m) is located 5 km east of Clermont-Ferrand and only 1.2 km north of the Grand Gandaillat quarry (Figs. 3A, 3E and 4D). This is one of the major curiosities of Lower Auvergne because of the bitumen lifts, formerly used to caulk boats and mark sheep. After decades of neglect, the site has been restored and is maintained by the Auvergne Conservatory of Natural Spaces. The Puy de la Poix mound, less than ten meters high, is a severely eroded Miocene volcanic chimney that crosses the Limagne marls. A ditch is filled with blackish bitumen and highly saline mineral water that oozes through the peperites. The salt concentration, which can exceed 80 g/l, varies greatly as a result of evaporation or dilution with rainwater. This water contains a distinct, non-mineralizing, microbial ecosystem.

(v) The Sainte Marguerite site is located 15 km southeast of Clermont-Ferrand (Figs. 3A, 3F, 4E and 4F). It corresponds to an abandoned thermal spa that is now only used to produce and bottle mineral water. There are many thermal springs in this region where water and gas, rich in hypogean (volcanic) CO_2 and Ca^{2+} ions, ascend. According to a local legend, this was the location where the Roman soldiers tended their horses during the siege of Gergovie in 52 BC, which preceded the final victory of Julius Cesar at Alésia (near Dijon) over the Gallic armies. The therapeutic virtues of these springs are currently still used and many people come to swim in Grand Saladis or drink the mineral water in Petit Saladis. The site is positioned on the southern part of the Limagne Basin along the Allier riverside (Fig. 3A). The presence of thermal springs is due to the close proximity to the volcanic "Chaîne des Puys" area, the underlying Oligocene limestone beds and the alteration of granitoids, causing the precipitation of travertine (Teboul *et al.*, 2016) with aragonite, calcite, Fe-rich gels and oxides. The springs in the Sainte-Marguerite area, such as the Saladis spring, were primarily studied to characterize the fluids merging from a fractured basement (water and gas composition, *e.g.* Gal *et al.*, 2012). Only petrographic and geochemical studies on the travertines associated with these hydrothermal vents have been published (Casanova *et al.*, 1999; Rihs *et al.*, 2000; Teboul *et al.*, 2016). Travertine precipitation occurs with a significant biological influence in gradually more distal or lower energy environments, as stated by Chafetz and Folk (1984) and Chafetz and Guidry (1999).

4 Fossil microbial deposits

4.1 Composition of the buildups

Buildup architectures were described according to the three commonly used scales (macro/meso/micro-fabric) according to Shapiro (2000). The macrofabric (or growth morphology) corresponds to the external shape of a single buildup. Five different macrofabrics of the buildups could be identified in the central and Bourbonnaise Limagnes basins (Roche *et al.*, 2018), and can be found in the Chadrat and Jussat area: (1) flats, (2) cauliflowers, (3) domes, (4) cones and (5) coalescent columns. Their main characteristics are summarized in Figure 9 and illustrated in Figure 10. The mesofabric is the internal organization of the buildups as can be observed with the naked eye. All of the morphologies present at these sites display a flat to columnar laminated mesofabric (*i.e.* none are clotted, ...). Finally, the microfabric refers to the smallest scale that can be distinguished with an optical microscope. Four microfabrics were defined by Roche *et al.* (2018). The three first are microbial-dominated: laminated (l), columnar (co), filamentous (f) and the fourth is a "coated-caddiflies" (cc) microfabric. All these microfabrics have been recognized in the different outcrops and used in this manuscript (see Figs. 11A–11H for illustrations). This classification

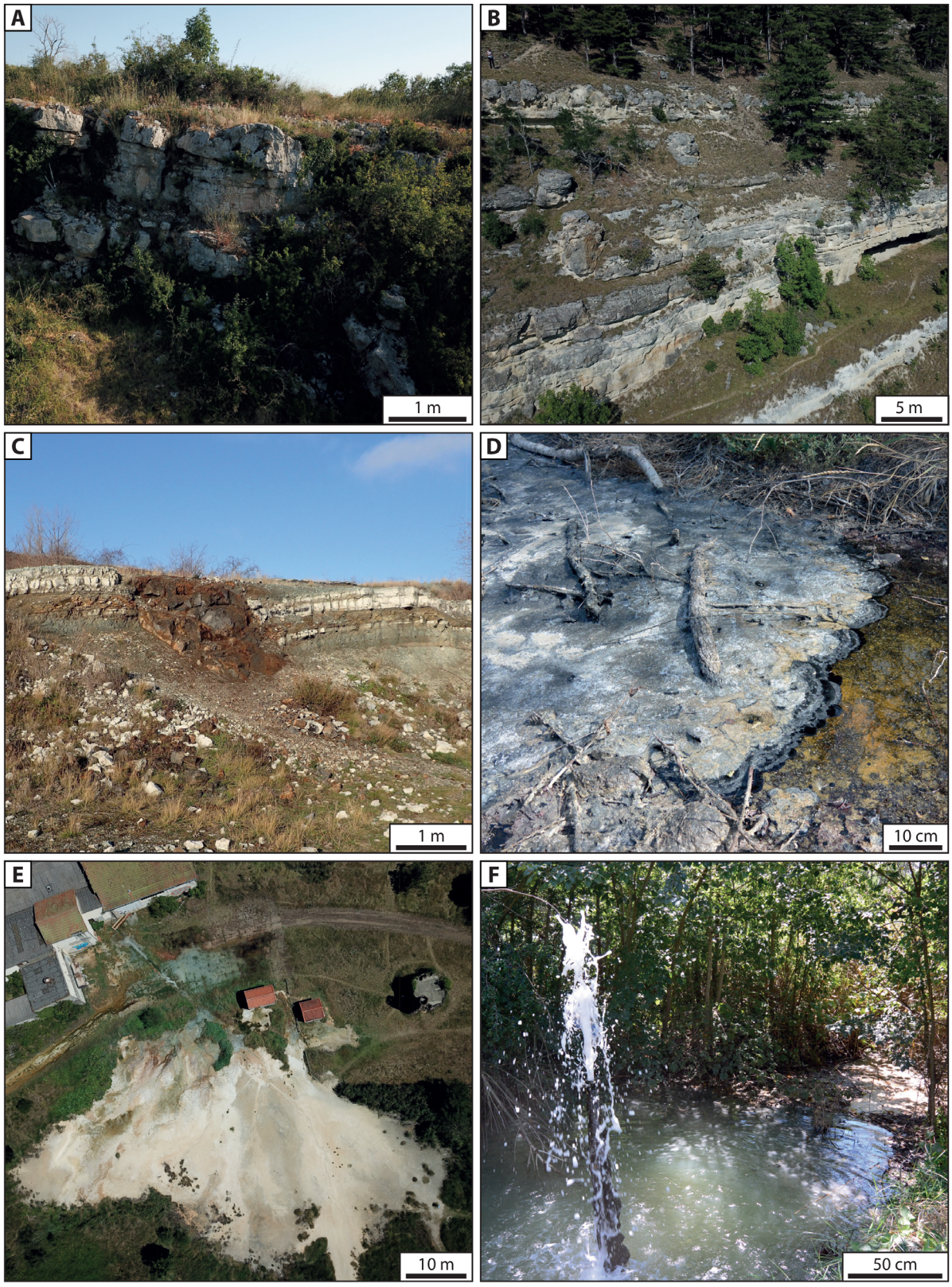

Fig. 4. Macroscopic views from the different visited outcrops and quarries (drone images acquisition by MAVIC PRO and DJI GO4): A. Drone acquisition from the Chadrat biostrome. B. Drone acquisition from the Jussat Outcrop showing the whole vertical section. C. Panorama of the Grand Gandaillat quarry showing the lacustrine and palustrine cycles and a peperite dyke crosscutting the lacustrine deposits. D. Puy de la Poix outcrop, where the bitumen is degraded by sulfate-reducing bacteria. The white deposit at the water-air interface is considered as colloidal sulfur. E. Drone acquisition from the Sainte Marguerite showing a large modern carbonate platform alimented by an outflow channel connected to the Chapelle well (behind the old bottling fabric). F. Water and CO_2 eruptions at the Geyser (see Fig. 3F for position).

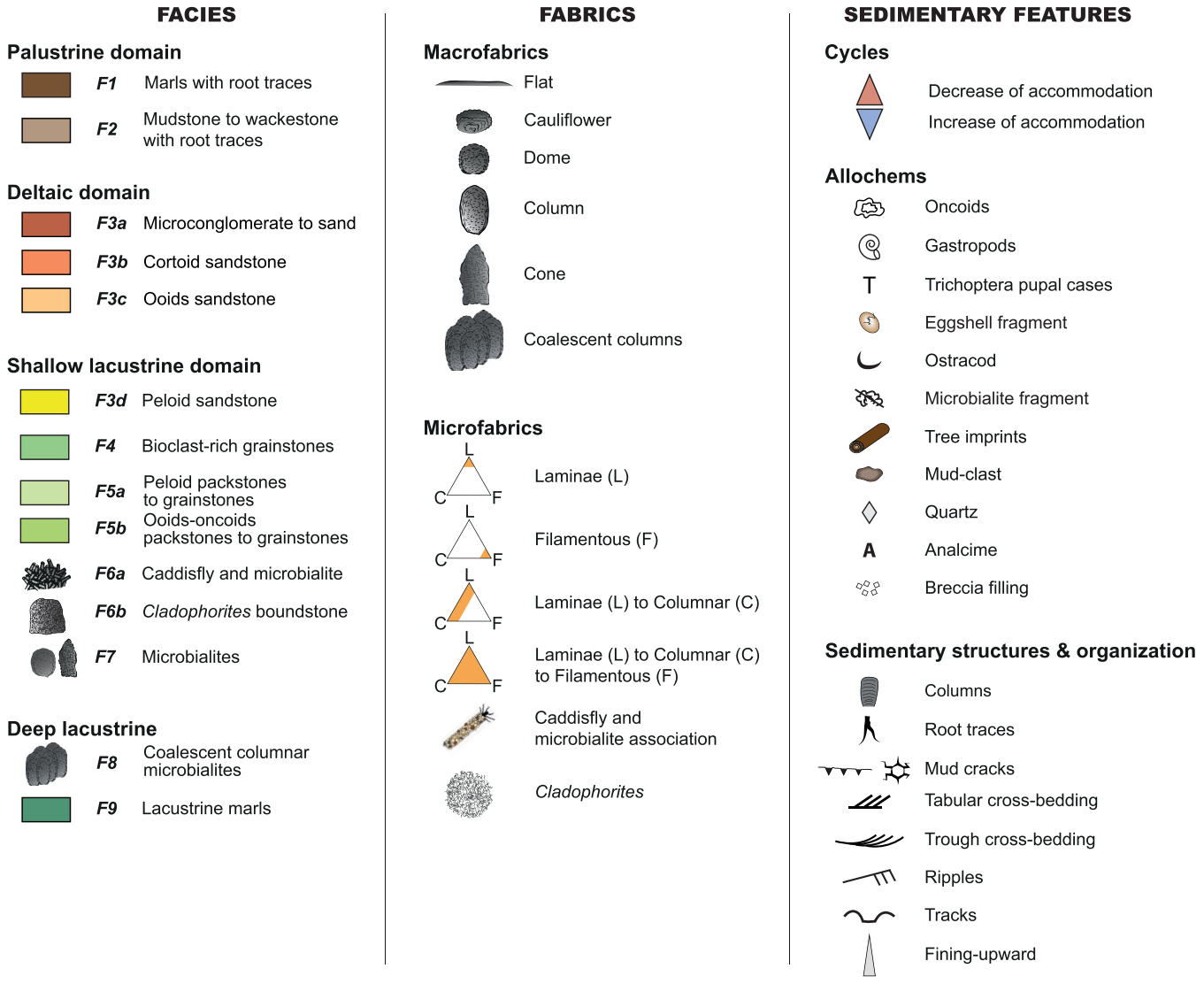

Fig. 5. Captions for Figures 6, 7, 8, 13, 16 and 17.

has been extended in including the textural features (*e.g.* micrite, cement, hybrid, biofeature, agglutinated; Fig. 9). However, in Chadrat and Jussat outcrops, the coated-caddiflies can be replaced in some microfabrics by *Cladophorites* (cl). In addition, the microfabrics are either micritic, cemented, composed of biofeatures or agglutinated and are characterized as hybrid when different microfabrics are associated (Fig. 11).

The Jussat and Chadrat buildups, are two neighboring outcrops and display similar morphologies and compositions as the ones observed in Créchy (Figs. 11A–11H), while they differ to those Grand Gandaillat (Roche *et al.*, 2018). The Grand Gandaillat buildups are mainly flat and cauliflower macrofabrics composed of laminated and columnar microfabrics (Figs. 5 and 8). The caddisfly pupal cases are entrapped in the microbial successive growth phases but remain rare (Figs. 11A and 11B).

The Chadrat outcrop mainly hosts flat macrofabrics. Individual layers are stacked to form flat to columnar laminated mesofabric organized in biostromes up to 5 m high and which extend laterally over several meters (Figs. 5 and 6). The microfabrics of the flat Chadrat buildups are mainly filamentous although they display a wide variety of morphologies (Figs. 5, 6I–6N, 11G and 11H). Using a morphogeneric approach, Freytet (2000) interpreted most of the microfabrics in the Limagne Basin, filamentous or not, as resulting from the activity of algae. However, their taxonomic affiliation remains questionable, especially for the structures referred to as *Broutinella arvernensis*. The molds of filament preserved in the carbonate buildups instead resemble modern cyanobacteria, thereby suggesting a microbial origin. However, there is still doubt regarding of the exact genetic attribution. The association with early sparitic precipitation indicates a possible combination of biotic and abiotic carbonate precipitation processes (Roche *et al.*, 2018). The coexistence of molds and spiritic precipitation makes it difficult to determine if the microbes were involved in the formation of the microfabric or if they were only permineralized. In this case, the term "hybrid" is particularly useful for referring to these structures, which combine both biotic and abiotic processes, especially when they

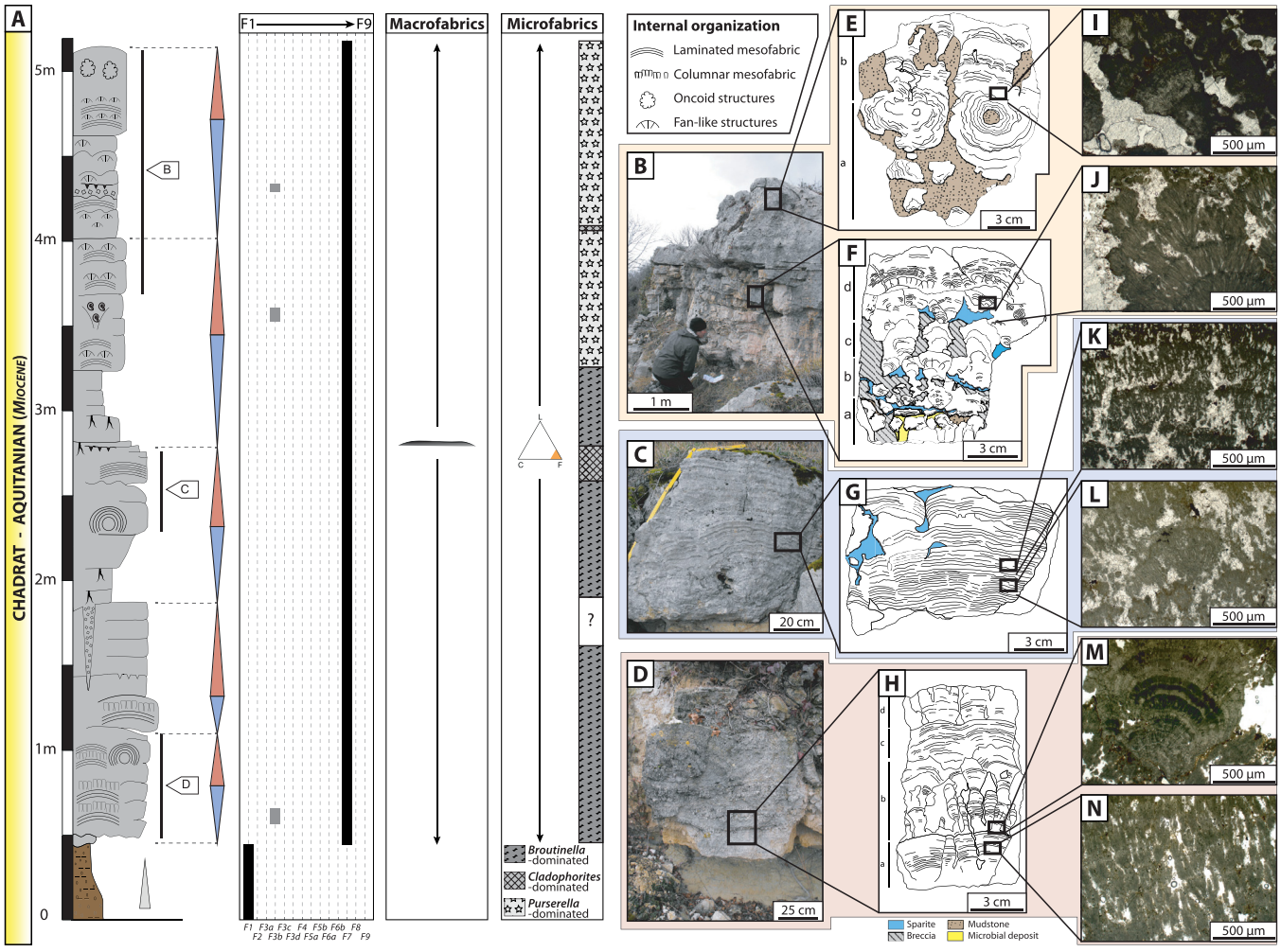

Fig. 6. A. Section of Chadrat with the lithology, cycle distribution (grey and yellow), facies, fabrics (macro and micro) of the buildups (see Fig. 5 for the captions, Supplementary Material, Table S1 for the detailed description of the facies and their depositional environments and Fig. 9 for information on the buildups). B–D. Macro and mesofabrics (see A for localization): B. Biostrome. C. Planar macrofabric and laminated mesofabric. D. Transition from marls to planar macrofabric. E. Oncoids embed in micrite (see B). F–H. Laminated to columnar mesofabrics (see B, C and D, respectively). I–N. Detail of the microfabrics (filaments identified by Freytet, 2000): I. *Plaziatella colleniaeformis*. J. *Purserella gracilis*. K. *Verrecchiella concinna*. L. *Cladophorites incrustata*. M. *Broutinella arvenensis*. N. *Broutinella ramulosa*.

are diagenetically overprinted (Riding, 2011; Vennin *et al.*, 2019; Riding and Virgogne, 2020). Hybrid microfabric corresponds to successive micritic and cement layers (Figs. 9 and 11E).

The Jussat outcrop displays the highest diversity in terms of carbonate buildups since five different macrofabrics and four microfabrics can be distinguished (Figs. 5 and 7) and can be compared with the fabrics observed in Créchy (Roche *et al.*, 2018). The macrofabrics are identical along a same horizon (lateral) and change only vertically. The core of the buildups corresponds either to an accumulation of caddisfly pupal cases (Figs. 11A and 11B) or *Cladophorites*; these two facies are never observed as being associated. The green algal (or cyanobacterial) genus *Cladophorites* is common in the central Limagne Basin (*i.e.* Chadrat and Jussat) and display filamentous microfabrics, encrusted by laminated planar cemented microfabrics (Fig. 11E). In the Limagne Bourbonnaise Basin, the occurrence of *Cladophorites* depends on the locality: this genus was observed in several quarries (Montaigu-le-Blin; Gondailly; Chavroches; Poncenat; Donsimoni, 1975; Wattinne, 2004) but was absent in Créchy.

4.2 Depositional environments of the central part of the Limagne Basin

Nine facies (F1 to F9) are described in detail in Table S1 and illustrated in Figure 12. They gather the microbial and metazoan buildups and the surrounding sediments of all of the visited outcrops. Three profiles of the palustrine and lacustrine ramp margin were identified in the central Limagne area (Fig. 13): two were published by Roche *et al.* (2018): Grand Gandaillat and Créchy, while a third, new, profile has been identified following the description of the Jussat outcrop. The different facies are organized into three or four depositional domains depending on the setting (Fig. 13): (1) palustrine, (2) deltaic (specific to the Jussat area), (3) shallow lacustrine and (4) deep lacustrine. The Chadrat deposits, which are only

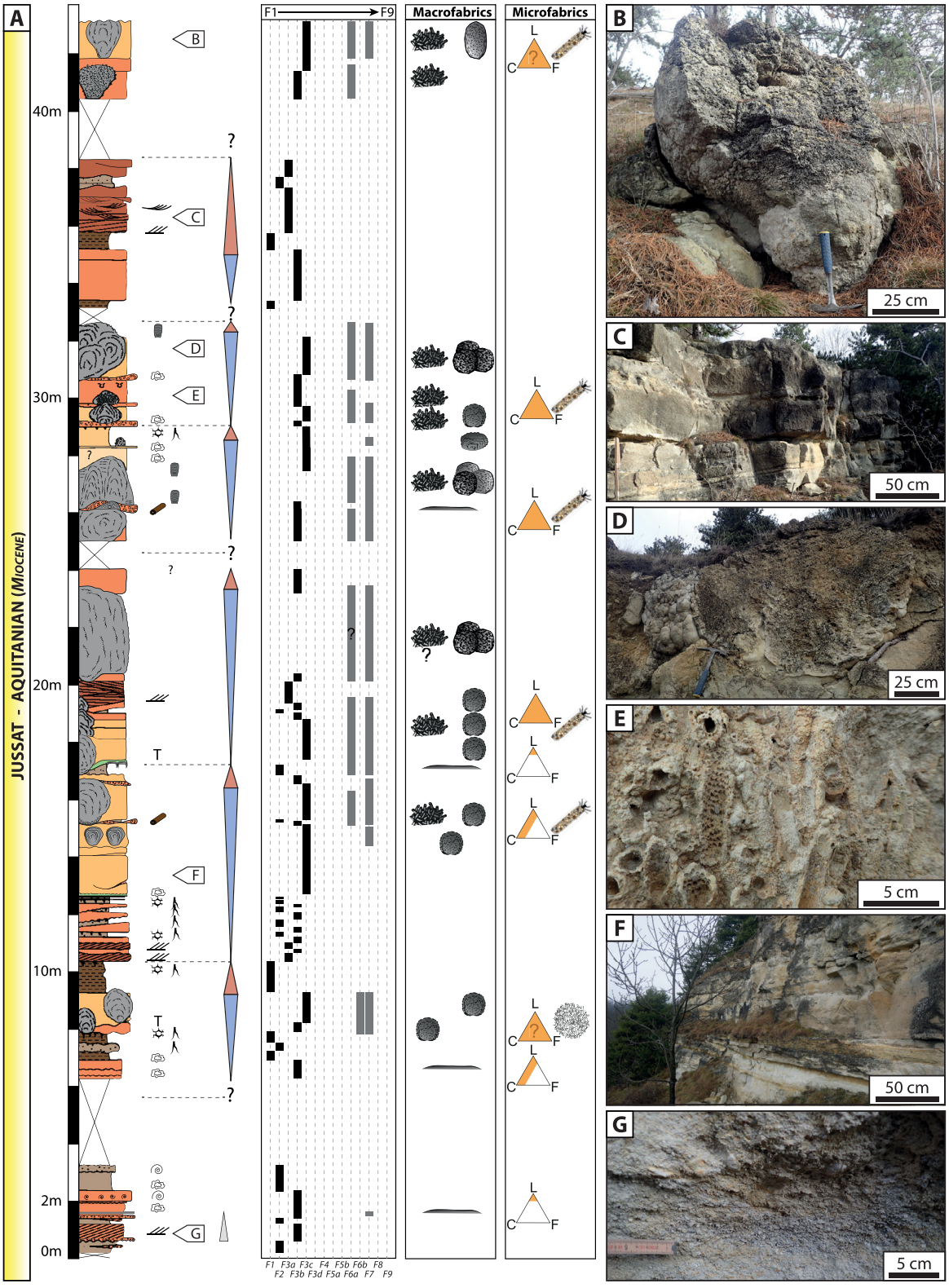

Fig. 7. A. Section of Jussat with the lithology, cycle distribution (grey and yellow), facies, fabrics (macro and micro) of the buildups (see Fig. 5 for the captions, Table S1 for the detailed description of the facies and their depositional environments and Fig. 9 for information on the buildups). B–G. Macro and mesofabrics (see A for localization): B. An eroded cone revealing its core, composed of massive caddisfly-rich cluster encrusted with microbial layers. C. Microconglomerate to sandstone with erosion channels on top and cross bedding. D. Coalescent domes composed of massive caddisfly-rich cluster and microbial-rich layers. E. Detail or caddisfly-pupal cases trapping gastropod shells. F. Large lenticular to lobate beddings composed of cortoid sandstones. G. Microconglomerate to arenite composed of quartz, carbonate grains and rare gastropods.

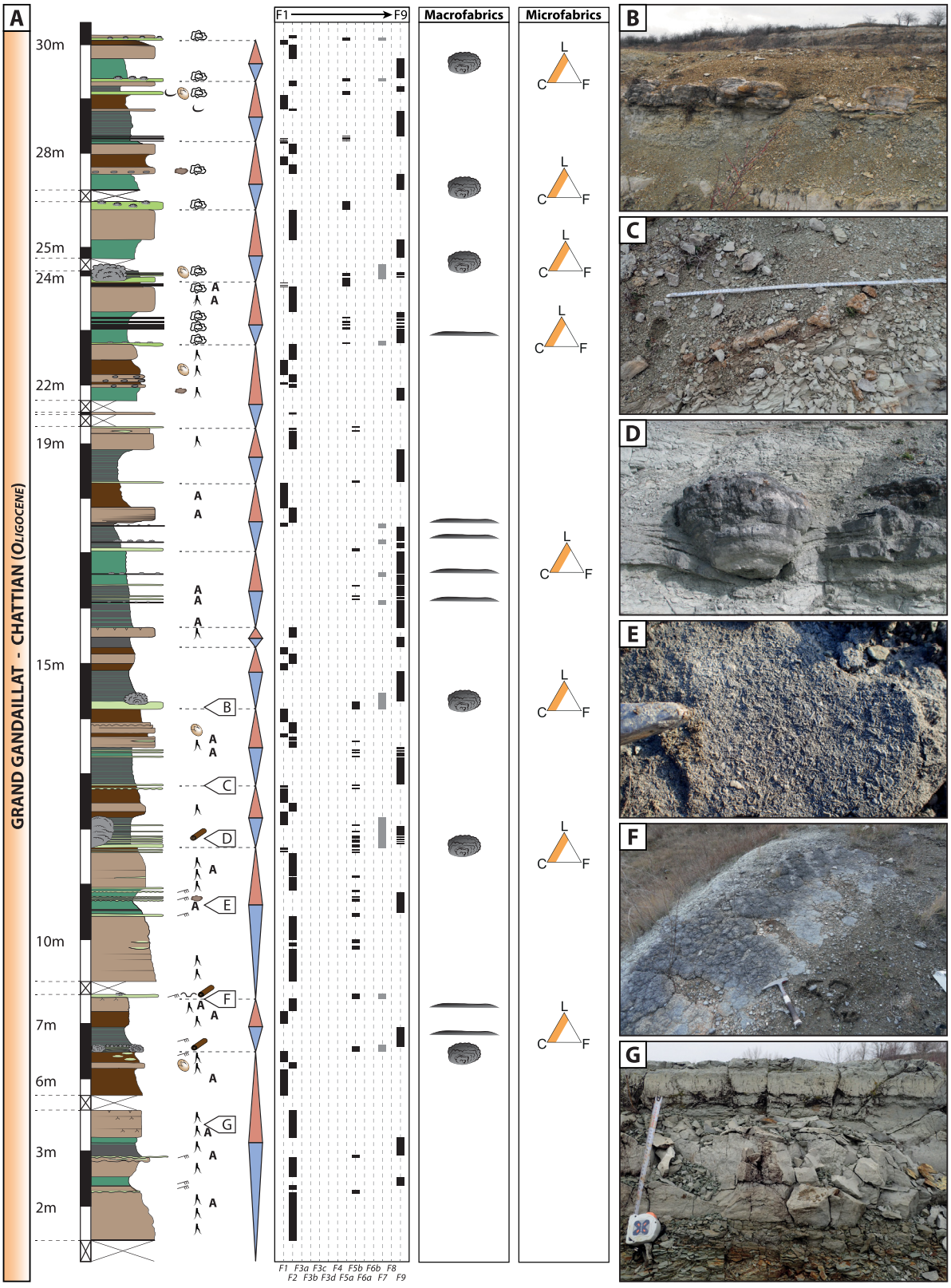

Fig. 8. A. Section of Grand Gandaillat quarry with the lithology, cycle distribution (grey and yellow), facies, fabrics (macro and micro) of the buildups (see Fig. 5 for the captions, 1 for the detailed description of the facies and their depositional environments and Fig. 9 for information on the buildups). B–G. Macro and mesofabrics (see A for localization): B. Cauliflowers organized in horizontal beds. C. Planar to wavy beds composed of microbial-rich deposits. D. Cauliflower developed on oncoid/ooid grainstone. E. Bioclastic-rich grainstone. F. Extended flat to planar microbial-rich crust. G. Mudstone with root traces (F2).

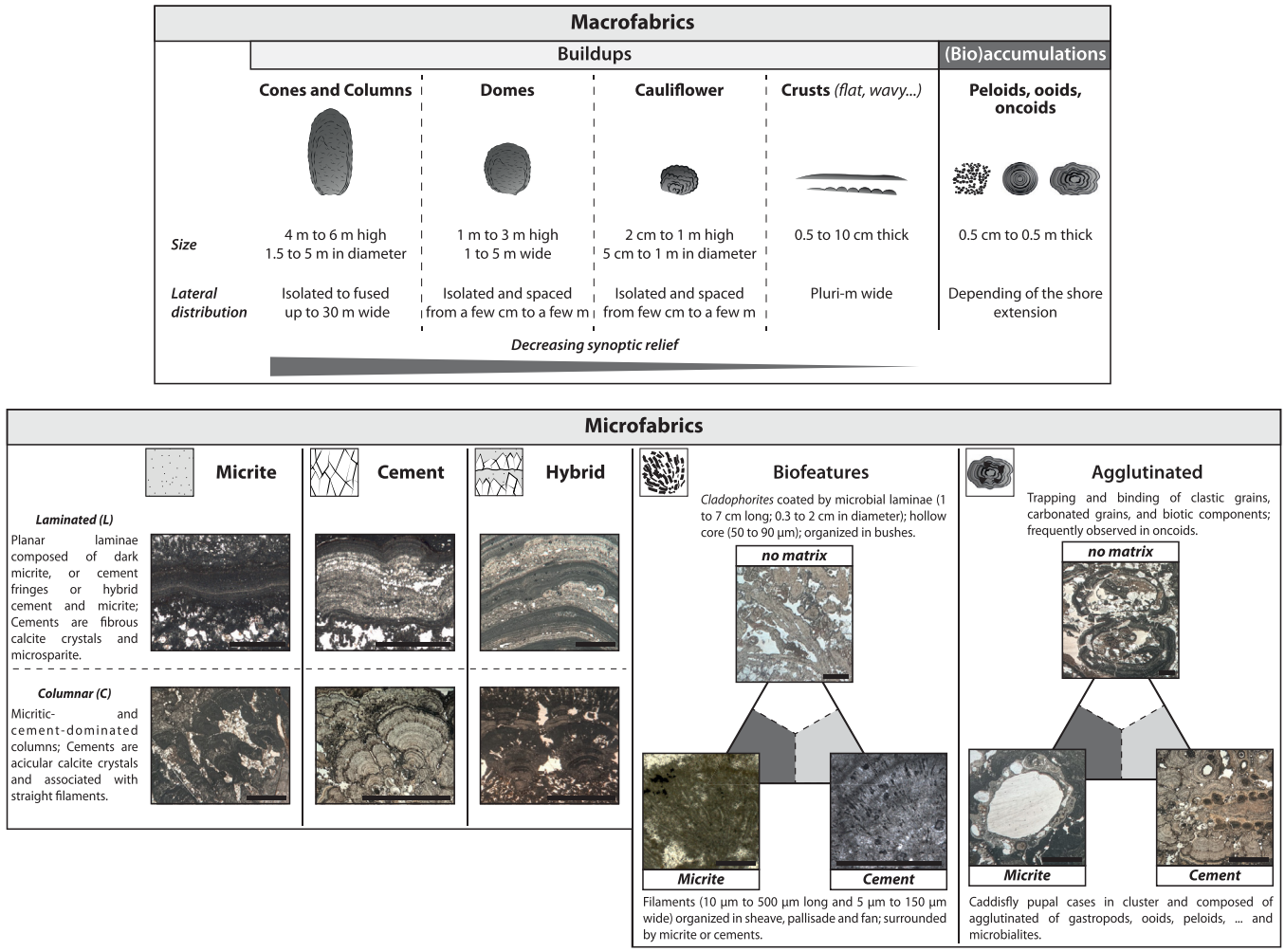

Fig. 9. Classification and description of the macro- and microfabrics deduced from the observation of the Oligo-Miocene buildups. Illustrations of microfabrics (Micrite: Jus-45 and jus17A: Cement: Jus-45 and Cre-36A; Hybrid: Jus-42 and Ch-5; Biofeatures: Jus-48A, Ch- and Jus-53A; Agglutinated: Jus-61; Jus-67; Cre36A).

shallow lacustrine deposits, are very similar to the F3 to F5 facies of Créchy (Roche *et al.*, 2018). Therefore, the Chadrat outcrop can be considered as equivalent to the proximal part of the Créchy ramp margin model.

4.2.1 Palustrine domain

This domain is mainly composed of palustrine marls (F1) and mudstones with roots traces (F2). These facies have been interpreted as palustrine deposits undergoing emersion and plant colonization (Roche *et al.*, 2018). In Chadrat and Jussat, emersion episodes are well expressed in form of desiccation cracks and orange-red colored mottled marks, glaebules and circumgranular cracks. The clay fraction is composed of iron-rich illite and kaolinite.

4.2.2 Deltaic domain

This domain, organized from proximal to distal deltaic environments, is only observed in the Jussat area (Figure Jussat Log). The proximal deltaic domain is characterized by a transition from the fluvial channel to the fan delta. The channels present basal erosion surfaces and are filled by microconglomerates to sandstones (F3a), passing laterally and vertically to palustrine marls (F1; Fig. 12A). The sandstones correspond to cm- to dm-thick lenticular beds with planar and oblique laminations. These deposits include quartzwackes (Pettijohn *et al.*, 2012) composed of moderately-sorted angular to sub-angular quartz grains (100 µm to several cm), extraclasts (angular quartzite fragments and rounded volcanic grains; mm to cm), feldspars, peloids and gastropods. Lakeward, the intermediate deltaic lacustrine domain is characterized by cortoid-rich sandstones (F3b) organized in m-thick prograding lenticular beddings (Figs. 12B and 12C). They present a lobate to cuspate morphology and comprise planar to oblique laminations. The sandstones embed cauliflower and domal buildups from the shallow lacustrine domain. The cortoid grains are angular to subangular poorly-sorted quartz grains (100 µm to several cm), and are associated with feldspars, peloids, gastropods, ostracods, microbial-rich

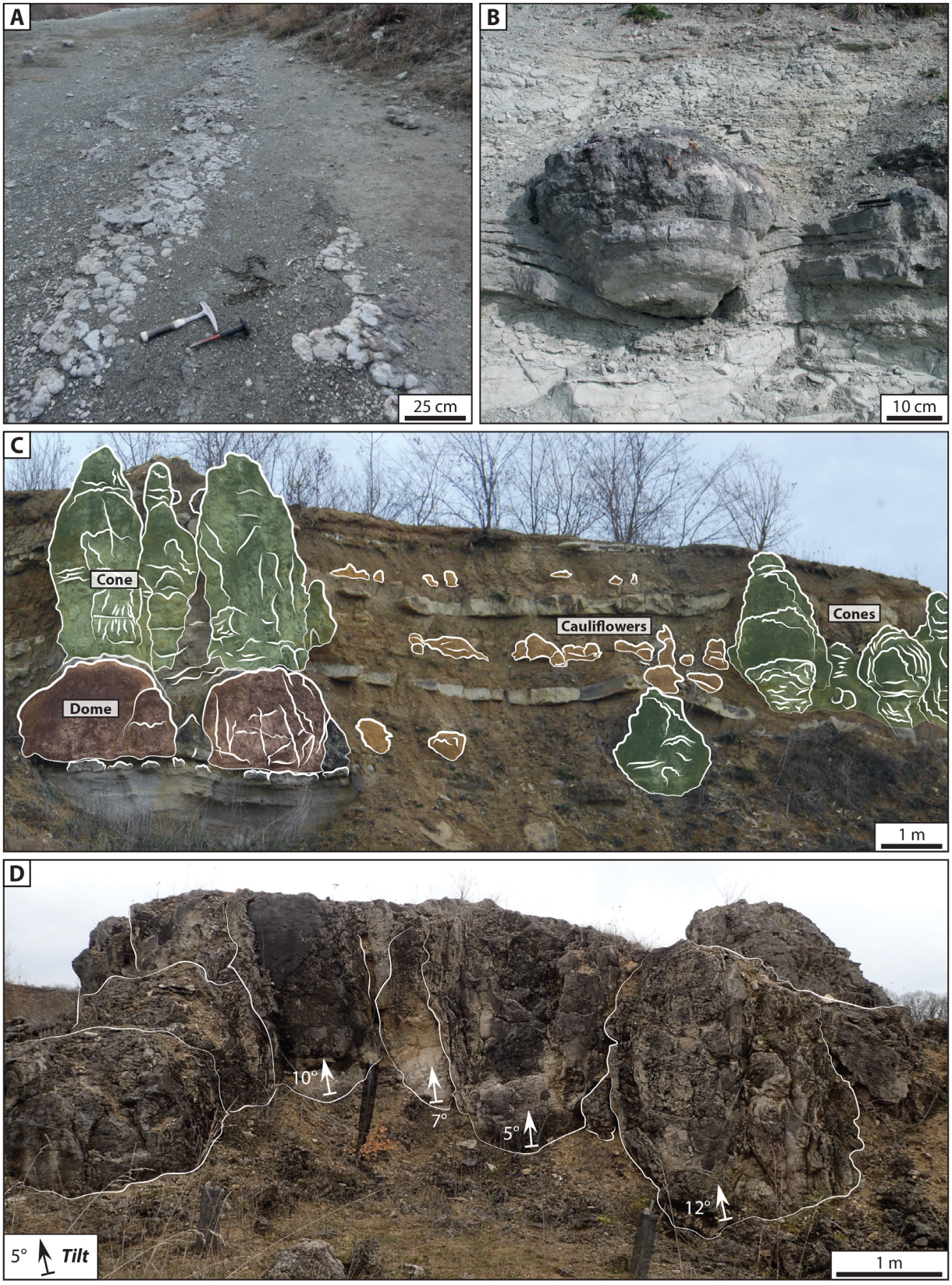

Fig. 10. Illustration of the microbial and metazoan buildups of the Oligo-Miocene visited outcrops and quarries following the classification for the macrofabrics. A. Flat macrofabrics (Grand Gandaillat quarry). B. Cauliflower (Grand Gandaillat quarry). C. Panorama of the Créchy quarry showing the relationships between the buildups and the surrounding marls and palustrine carbonate deposits; Domes passing upward to cones. D. Coalescent columns inclined in an ENE direction (Créchy quarry).

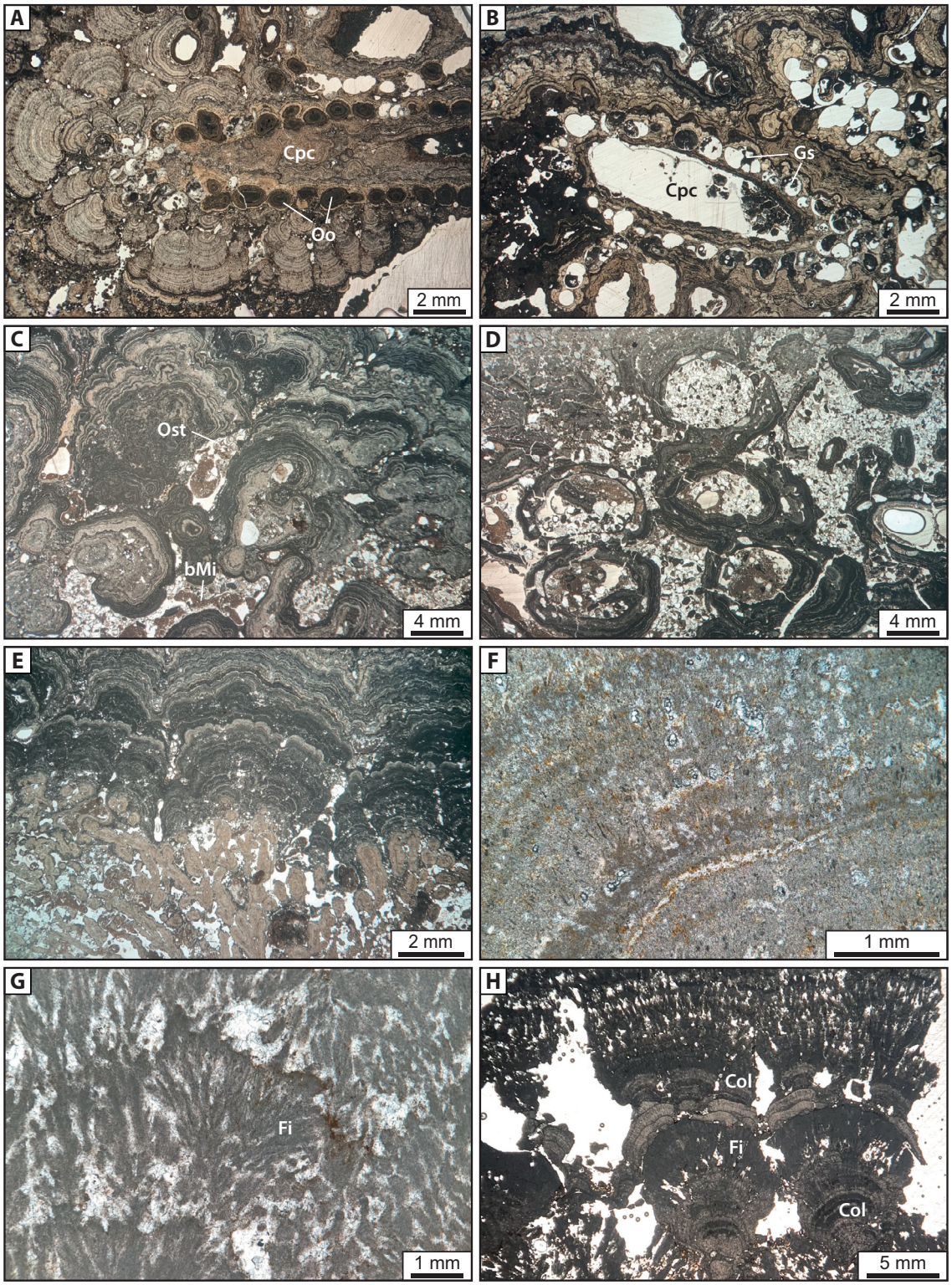

Fig. 11. Thin section illustrations characterizing the microfabrics of the microbial and metazoan buildups (see Fig. 9 for description and classification and Figs. 6, 7 and 9 for position). A. Cross-section of the caddisfly pupal cases trapping ooids (Oo) and encrusted by *Broutinella avernensis* (Jus-64). B. Cross-section of the caddisfly pupal cases (Cpc) trapping gastropod shells encrusted by microbialites (Gs; Cre-36A). C. Microbialites developed upon clastic sands showing very low trapping of quartz during microbial growth (Jus-61); Cavity are infilled by a brown micrite (bMi) and ostracods (Ost). D. Coalescent oncoids embedded in clastic sands and trapping grains (Jus-61). E. Transition from cluster of *Cladophorites* to microbialites showing an alternance of cement and micritic layers (Jus-48A). F. Microbialites showing an alternance of laminated cement and micritic microfabrics (Jus-53A). G. Successive layers composed of filaments (Fi) embedded in micrite and microsparite (Ch-21). H. Dark micrite-dominated laminae stacked to form column (Col) and dense filament-rich layers (Fi; Ch-5).

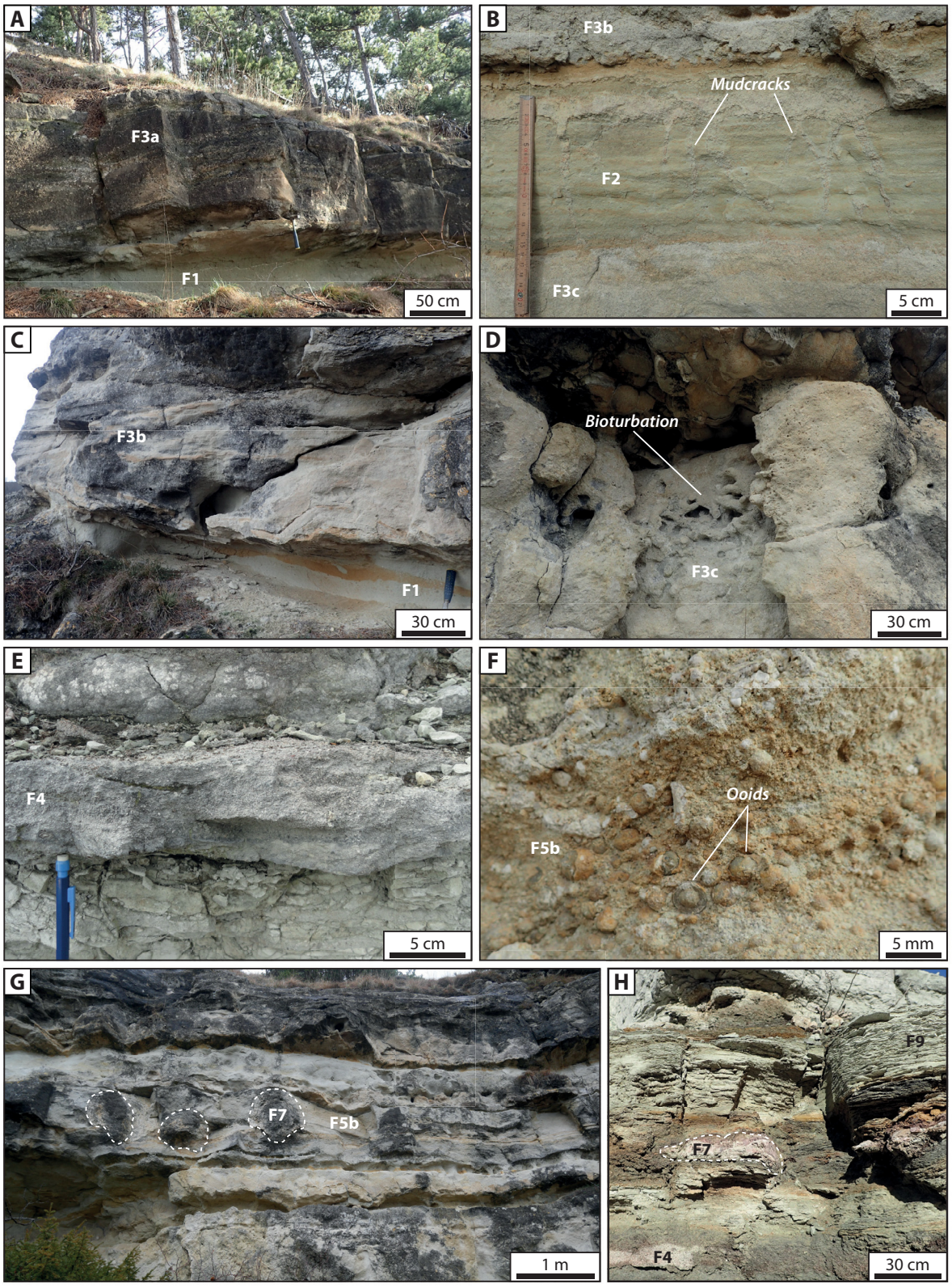

Fig. 12. Illustrations of the main sedimentary facies. A. Channels infilled by clastic sandstones and crossed lamination eroding marls (F1; Jussat). B. Mudstone with root traces and mudcracks (F2; Jussat). C. Large lenticular to lobate layers showing through cross bedding (F3b; Jussat). D. Bioturbated ooid-rich sandstone (F3d; bioturbation resembling to Egbellichnus jordidegiberti igen. and isp. nov.; Jussat outcrop). E. Bioclastic-rich grainstone showing ripples (F4; Grand Gandaillat quarry). F. Oncoid-rich packstone to grainstone (F5b; Jussat). G. Metre-high microbial-rich domes (F7) embedded in a peloid/ooid-rich packstone (F5b; Jussat). H. Cauliflower (F7) evolving to marls composed of organic matter-rich clay layers (F9; Grand Gandaillat).

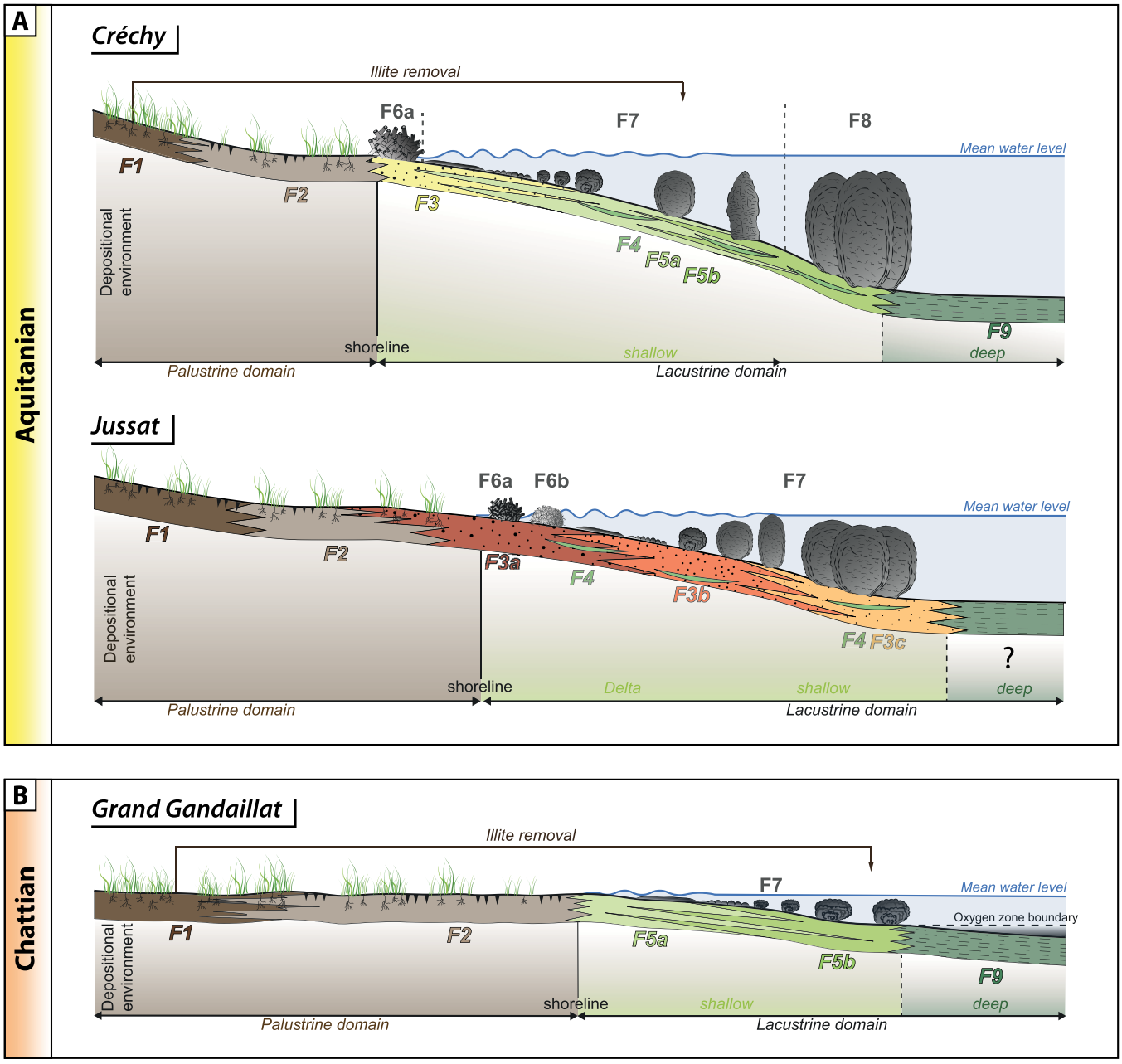

Fig. 13. Reconstitution of the Palustrine to lacustrine depositional environments: (A) Aquitanian high-gradient margin model with a carbonate-dominated sedimentation at Créchy and Aquitanian high-gradient margin model closed to deltaic influences at Jussat. (B) Chattian low-gradient margin model at Grand Gandaillat.

fragments and extraclasts (angular quartzite fragments and rounded volcanic grains; mm to cm). Locally, dm-thick layers composed of conglomerates, wood fragments and gastropods *Cepaea Moroguesi* (Rey, 1971; Hugueney *et al.*, 2003) are preserved at the base of the sandstones. In the distal part, the deltaic domain (or prodelta) is made up of ooid-rich sandstones (F3c). This facies is organized in cm- to dm-thick planar beddings and mainly formed by an accumulation of ooid (quartz nuclei) and quartz grains. It is associated with oncoids (50–500 μm), cortoid grains, peloids, gastropods, ostracods and rare extraclasts. The grains are embedded in a micritic matrix. Bioturbation that resembles the Late Miocene ghost shrimp Egbellichnus jordidegiberti igen. and isp. nov. has also been evidenced (Fig. 12D; Hyžný *et al.*, 2015).

In lakes, the geometry and sedimentary characteristics of deltas are controlled by the tributaries (rivers) and waves/currents dynamics of the waterbody (Galloway, 1975). The angular shape and moderate sorting of the quartz and feldspar grains in F3a suggest a low transportation distance from the source area. The lenticular beddings, oblique laminations, the coarse sandstones and conglomerates are interpreted as fluvial deposits deposited under high energy flow (*e.g.* Yemane *et al.*, 1989; Platt and Wright, 1991; Olariu and Bhattacharya, 2006; Mtelela *et al.*, 2016; Zhu *et al.*, 2017). Similar deposits have been observed in the lacustrine margin (Yemane *et al.*, 1989; Platt and Wright, 1991) and ephemeral fluvial channels (Scherer *et al.*, 2007). The lacustrine part of the deltaic environment presents a lobate to cuspate morphology and is frequently shaped by waves as observed in Lake Turkana (Kenya; Schuster and Nutz, 2018). In marine environments, cortical grains are attributed to light-dependent, perforating microorganisms and usually form below the fair-weather wave base (Flügel, 2004). In contrast, cortical grains are poorly described in lakes, and in these environments interpreted as deposited under high-energy conditions (Fedorchuk *et al.*, 2016; Platt and Wright, 1991). The presence of fragmented clasts, isolated ostracod valves and cross-bedding observed in the Jussat deltaic sediments in association with cortical grains support high-energy conditions (*e.g.* Yemane *et al.*, 1989; Olariu and Bhattacharya, 2006; Zhu *et al.*, 2017). In addition, the layers composed of conglomerates, wood fragments and gastropods *Cepaea Moroguesi* (Rey, 1971; Hugueney *et al.*, 2003) indicate flooding events which have reworked material from the continental settings. Ooids are also associated with high-energy, shallow, lake environments (Eardley 1938; Swirydczuk *et al.*, 1979; Tucker and Wright 1990; Bouton *et al.*, 2016); the presence of ripples and reworked grains in ooid deposits argues for wind-generated resedimentation (Blair and McPherson 2008). The transition to fine material and increasing bioturbation is interpreted as a prodelta area where fine material settles out of suspension (Middleton *et al.*, 2005). The ichnotaxon identified in the sublittoral deposits of Lake Pannon (Slovakia; Hyžný *et al.*, 2015) can be used to confirm the subaquatic interpretation.

4.2.3 Shallow lacustrine domain

The shallow lacustrine domain is composed of six facies: sandstones (F3d), bioclastic-rich grainstones (F4), peloid/ooid-oncoid pack-grainstones (F5), microbialites associated with caddisfly pupal cases (F6a) and *Cladophorites* (F6b) and microbial-rich facies (F7). Most of these facies have been described in Roche *et al.* (2018) and are summarized in Table S1 and illustrated in Figure 12. The Jussat and Chadrat sedimentary records differ from that of Grand Gandaillat by the presence of gastropod and/or ostracod accumulations that are slightly encrusted by microbialites (F4: Fig. 12E; F5 a and b: Fig. 12F). The caddisfly and microbialite facies (F6a) correspond to clusters of caddisfly pupal cases. The caddisflies were attributed to Phryganeidae or Limnephilidae by Hugueney *et al.* (1990). *Cladophorites* were identified for the first time by Bertrand-Sarfati *et al.* (1966). They contributed to the development of cylindrical, bushy masses, 30 to 50 cm in diameter and 10 to 50 cm in height, with internal centimetric laminations (F6b). The algae are encrusted by *Broutinella arvernensis* (Freytet, 1998, 2000), which favors the preservation of these fragile structures. Most of the microbial-rich facies (F7: Fig. 12G) include the same morphologies as those described in Créchy and Grand Gandaillat (flat, cauliflower, dome and cone macrofabrics; Roche *et al.*, 2018). The microbialites are frequently affected by penetrative dissolution, with cavities infilled by gastropod and ostracod grainstones (facies F4). In Chadrat, the built facies are frequently crosscut by root traces and fissure cracks.

The shallow water environments of the lake can be identified from a characteristic presence of caddisfly pupal cases, indicative of shallow conditions (Mackay and Wiggins, 1979; Leggitt and Cushman, 2001; Leggitt *et al.*, 2007). *Cladophorites*, considered to be the equivalent of the current green algae *Cladophora* (Freytet, 2000) or cyanobacteria are also associated with shallow lake environments, developing in fresh to brackish waters (Riding, 1979; Arp, 1995). Similar environmental conditions have been proposed in the northern part of the Limagne Basin (Wattinne *et al.*, 2003) and the Reis impact crater (Germany; *e.g.* Reis, 1921; Riding, 1979; Christ *et al.*, 2018). The maximum water level elevation is estimated from the maximum vertical development of the microbialites without interruption during their growth, until the formation of an erosion or emersion surface, *i.e.* when the buildups reach the lake surface (Bouton *et al.*, 2016; Roche *et al.*, 2018; Vennin *et al.*, 2019). These observations reinforce the hypothesis that the water column has probably never exceeded the height of the bioconstructions (in Jussat: 3 to 4 m and in Chadrat: < 1 m) and attest to rapid water level fluctuations. Features such as highly fragmented biotic content, shell accumulation, the composite nature of the components, oblique laminations, ripples and erosional surfaces, as well as the truncation of some microbial deposits suggest a wave-influenced high-energy depositional environment (Schuster and Nutz, 2018).

The different macrofabrics of the bioconstructions may evidence local differences in the hydrodynamic regime. In Chadrat, the flat macrofabrics and the preservation of the micritic matrix suggest low-energy conditions. The presence of dissolution surfaces, karstification and/or pedogenic features affecting the bioconstructions seem to indicate a fluctuating water level up to their exposure following emersion. Cauliflowers, domes and columns form under moderate to high-energy conditions as they are associated with packstones, grainstones and sandstones in the Jussat area. The development of microbial-rich carbonate deposits, lacking of a fine clastic component, may result from (i) a rapid increase in the water level, (ii) a fast growth of the bioconstruction supported by a high calcium carbonate precipitation rate,

(iii) permanent hydrodynamics preventing the deposition of fine particles in shallow domains and/or (iv) the presence of vegetation in the littoral zone which traps fine sediments and protects them from removal (Koinig *et al.*, 2003). In the fan delta of Jussat, an environment which usually carries consequent loads of clastic particles, the absence of clastic components entrapped in the microbialites during their growth suggests changes in the inputs, and thus to the terrestrial run-off conditions.

4.2.4 Deep lacustrine domain

The deep lacustrine sedimentation is characterized by coalescent columnar microbialites (F8) and lacustrine marls (F9: Fig. 12H). In the central Limagne Basin, lacustrine marls were only observed in Grand Gandaillat, and in association with the highest domes and columns in Jussat. They were absent from the Chadrat outcrop, only representing a shallow lacustrine domain. The lacustrine marls are interpreted as low-energy, organic matter-rich marls deposited in the deep parts of a shallow lake (Roche *et al.*, 2018). In Jussat, the synoptic relief of the coalescent columns is limited to 3–4 m when they reached the lake surface (emersion surfaces have been observed on top of each individual dome).

During the Aquitanian, the Jussat and Chadrat area corresponds to shallow environments close to the shoreline. By contrast, Créchy quarry records deeper and more distal conditions as evidenced by the higher synoptic relief of the coalescent columns and the widespread lacustrine marls. In addition, the deltaic environment characterized in Jussat argues for its proximity to the mouth of a perennial river.

5 The modern microbial deposits

Modern microbial mats can be found in different locations in the Limagne Basin (*e.g.* Sainte-Marguerite, Source de l'Ours, Serra *et al.*, 2003). Contrary to the Cenozoic bioconstructions, which were lacustrine, the most spectacular modern examples are associated with thermal spring environments. Although modern microbial deposits do not represent exact equivalents of the Limagne fossil systems, they offer an opportunity to understand the role microbial communities play in the precipitation of carbonates. The Sainte Marguerite thermal spring is one of the 22 springs referred to on the edge of the Limagne Basin (Serra *et al.*, 2003). A fan-shaped flat mound forms at the outflow of the spring. This mound extends over 100 hundred square meters and constitutes a synoptic relief of a few centimeters to decimeters (Fig. 4E). The water flows downslope where iron oxides and carbonate shrubs precipitate close to the source and calcite and aragonite-rich layered deposits are present in the distal part of the fan (Fig. 14A). Benthic microbial communities (biofilms of cyanobacteria, and diverse population of other bacteria and archaea) and eukaryotes (diatoms and chlorophytes) colonize the shallow pools of the fan-shaped mound (Figs. 14A–14C) and can be linked to carbonate deposition (Figs. 14C–14G; Casanova *et al.*, 1999). The diverse cyanobacterial populations can be observed by differential interference contrast microscopy (Olympus FluoView FV1000) and confocal laser scanning microscopy with an oil immersion objective (Olympus UPSLAPO 60×0). The prototrophs in the mat are composed of species resembling *Lyngbya* sp. (Figs. 15A and 15B), *Spirulina* sp. (Figs. 15B and 15C) and undetermined 5–8 mm long filamentous cyanobacteria, similar to *Phormidium incrustatum* as well as several diatom species (Fig. 15B). The main mineralized structures display stacked porous spongy laminae with erect fibrous micritic threads (15–20 μm) separated by micritic films (Casanova *et al.*, 1999). Between the filaments and the diatoms (Fig. 15D), the fabric observed in scanning electron microscopy (SEM; JSM-IT100, JEOL Ltd, Tokyo, Japan) is composed of micro-peloids (Fig. 15E), triangular masses (Fig. 15F) and nanospheres (Fig. 15G). The micritic laminae are wavy to crenulated, locally with mm-high domal forms. These mini-domes are intercalated with wackestone to grainstone and include coated bubbles (Figs. 14C–14E and 14G). The coated bubbles are spherical structures measuring several μm to 1 cm in diameter have a hollow core and a very thin micritic coating covering the surface (Figs. 14D and 14E). Coated bubble accumulations occasionally are associated and are either included within a micritic matrix or, alternatively cemented by fibrous crystals (Figure S1). The mineralogy of the coated bubbles was determined by FTIR spectroscopy and revealed a main composition of aragonite and calcite (Figure S2). The coated bubbles were cast in LR-white resin then cut and polished for micro-characterization using SEM. Secondary electron images showed that the walls of the coated bubbles are composed of several micrometer-thin layers with various morphologies (Fig. 15H and Figures S1A–S1G). Outer layers are made of needle-like (Figure S1B) and rosette-shaped crystals (Figure S1C). The inner layer part of the bubble surface is composed of hemispherical radial needle crystals (Figures S1D–S1F). Locally, carbonate paper-thin carbonate rafts, a few μm thick and up to several centimeters wide (Fig. 14F), accumulated in close proximity to the coated bubbles.

Coated gas bubbles form preferentially in travertine ponds, on shallow channel sides, and also in spring mounds (Ries Crater, Pache *et al.*, 2001; Big Soda Lake, Rosen *et al.*, 2004). The paper-thin rafts are submillimeter-thick carbonate films precipitating on the surface of stagnant pools. Both coated gas bubbles and rafts are common facies of hydrothermal travertines (Jones *et al.*, 1989; Taylor *et al.*, 2004; Della Porta, 2015) and form in low-energy depositional environments. The laminated micritic facies is related to the microbially-induced precipitation of microbial mats (Visscher *et al.*, 1998; Dupraz *et al.*, 2009; Bouton *et al.*, 2016; Pace *et al.*, 2018). The development of this travertine facies is thought to result from alternating humid periods with high energy flow and an evaporative period leading to low-energy flow (Rodríguez-Berriguete and Alonso-Zarza, 2019). It remains difficult to distinguish between biotic and abiotic processes of mineralization in microbial mats, especially in a travertine system, and is the focus of ongoing work in the Limagne Basin. Cyanobacteria present at the surface of the microbial mats and degassing of CO_2 may both trigger mineralization, biotically in the first case (Dupraz *et al.*, 2009) and abiotically in the second. If so, microbial mats may be site of the nucleation encrustation and considered as a biologically-influenced mineralization process (Merz-Preiß and Riding, 1999; Dupraz *et al.*, 2011).

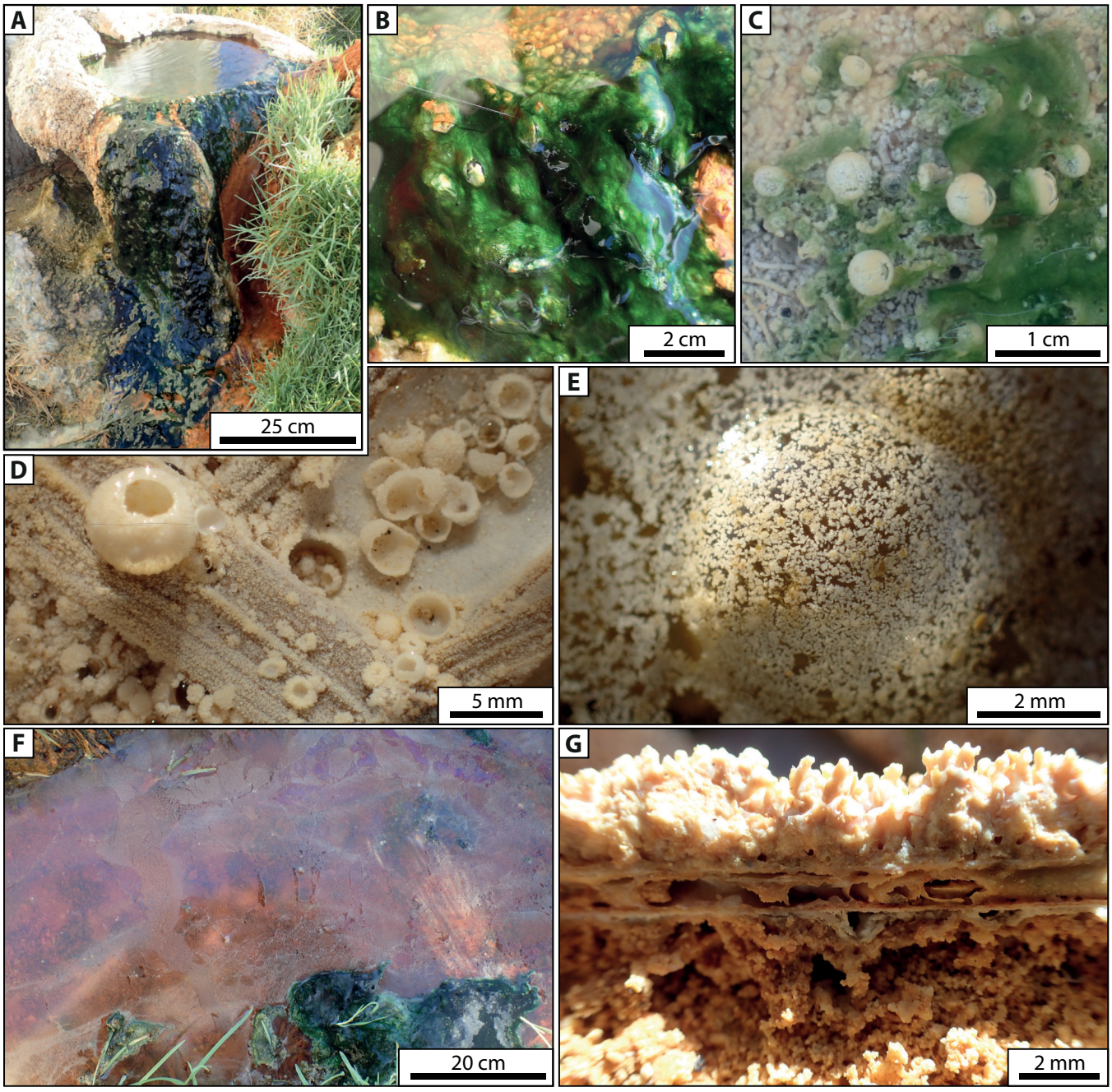

Fig. 14. Illustration of the main microbial structures and carbonate precipitates in Sainte Marguerite area. A. Microbial communities developed close to the spring in a reservoir. B. Microbial mats and filamentous cyanobacteria forming a biofilm of extracellular polymeric substances (EPS). C. Aragonite bubbles and associated microbial mats. D. Detail of the mineralization on blade of grass and aragonite preserved bubbles. E. Aragonite mineralization at the surface of a bubble. F. Aragonite raft at the air-water interface along the stream. G. Detail of the growing phase resulting from the mineralization in the carbonate system with erect fibrous micritic threads (15–20 μm) separated by micritic films.

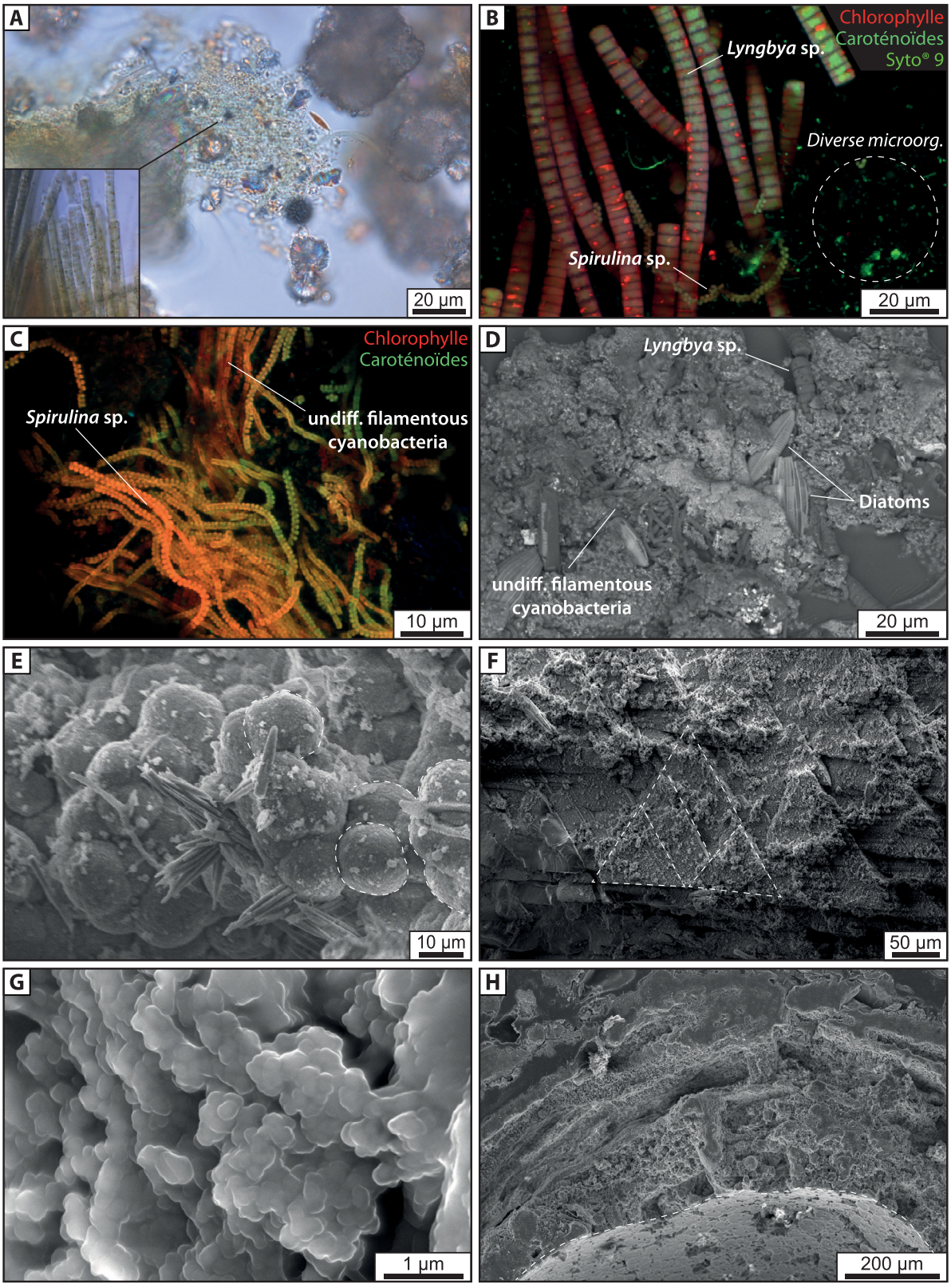

Fig. 15. A. Illustration of diatoms, cyanobacteria and minerals by differential interference contrast microscopy. B. *Spirulina* sp., *Lyngbya* sp. and divers micro-organisms by confocal laser scanning microscopy. C. Illustration *Spirulina* sp. and undetermined filaments by confocal. D–H. SEM images of golden-coated samples of: (D) Carbonates composed of nanospheres (zoom on photo G) precipitated close to diatoms and filamentous cyanobacteria (white arrow): (E) Micro-peloids of carbonates formed close to diatoms; (F) Trigonal microfabric of carbonates; (G) Nanospheres of carbonates; (H) Cross-section of cut and polished coated bubble included in LR-White resin.

The Puy de la Poix mound contains a very particular microbial ecosystem, a so-called "sulfuretum" (Baas-Becking, 1925), which is based on sulfur cycling (Fig. 4D). In this bitumen and saline, sulfate-rich water system, two main microbial populations dominate: (1) sulfate-reducing bacteria, which respire sulfate instead of oxygen and couple this to the oxidation of long chain hydrocarbons present in the bitumen to gain energy (Rosenfeld, 1947). In this process, hydrogen sulfide (visible as gas bubbles) is produced; (2) sulfide- (and/or reduced sulfur-) oxidizing bacteria convert the hydrogen sulfide to sulfate, with an intermediate accumulation of zero-valent sulfur (Megonigal *et al.*, 2003; Hines *et al.*, 2007). This zero-valent sulfur forms the whitish precipitate at the water-air interface. No specific mineralization processes have been observed linked to the metabolism of the microbial communities, although sulfur cycling can result in carbonate precipitation (Visscher *et al.*, 1998).

6 Discussion

This discussion summarizes the main controlling factors that were involved in the formation, development and transformation of the microbial deposits in fossil and modern examples of the Limagne Basin. Some of the controlling factors have been extensively discussed in Roche *et al.* (2018); however, new outcrops of Jussat and Chadrat provide additional information to better constrain the depositional environments. In addition, the modern microbial-rich systems visited during the 2019 meeting emphasized the importance of microbially-mediated carbonate precipitation. This information can be used to better approach the mineralization processes involved in the fossil deposits.

6.1 Depositional environment models

The lateral and vertical distributions of the facies in Jussat and Chadrat can be used to propose a 3D depositional model that gathers the sedimentation zones of the two areas. This model is proposed considering that both outcrops are contemporary (Aquitanian). However, to validate this hypothesis, palynological, mammalogical data or stratigraphic correlations should be refined. A synthesis of the 2D deposition models illustrating all of the visited outcrops (Chadrat, Jussat and Grand Gandaillat) and the northern Limagne Basin is proposed in Figure 13. All three of these Oligo-Miocene outcrops depict the same general cycle pattern evolving from palustrine to lacustrine domains. However, the three settings differ from each other in terms of the composition and size of the buildups, the respective thicknesses of the palustrine- and lacustrine-related sediments and the clastic inputs.

The 2D depositional model is based on the Grand Gandaillat outcrop and illustrates the Chattian sedimentary dynamics (Fig. 13B). During this period, the lake presented a flat margin profile which leads to the formation of microbial buildups with a low synoptic relief. Cauliflowers are the main microbial macrofabric encountered in the restored quarry and do not exceed 1 m in height. They pass vertically and laterally to lacustrine marls enriched in organic matter (Roche *et al.*, 2018). The two other 2D models illustrate the Aquitanian sedimentation in Créchy and Jussat and they display the same succession of carbonate facies (Fig. 13A). The Jussat area differs mainly by higher clastic sediments consecutive to the development of a lacustrine fan delta in association with the development of microbial and metazoan buildups (Fig. 13A). The flat and cauliflower macrofabrics form in the shallowest part of the lacustrine domain and record a high-frequency water level fluctuation as indicated by the presence of successive emersion surfaces and pedogenesis overprints. Lateral or vertical variations of the macrofabrics illustrate changes in the hydrodynamics: flat macrofabrics thrived under low-energy conditions whereas cauliflower macrofabrics developed under stronger energy conditions. In addition, the morphology and size of the cauliflowers result from the evolution of the sedimentation rate, accommodation (Wattinne *et al.*, 2003) and the nature of the substrate on which they developed (Vennin *et al.*, 2019). The Chadrat outcrop only presents the very shallow marginal settings of the lake, protected from clastic inputs. The stacking of flat macrofabrics, ultimately forming a biostrome, attests to a shallow lake environment (water depth less than 1 m). The presence of many root traces and karstified surfaces within the biostrome suggests that the area was regularly subjected to exposure and colonization by vegetation. By contrast, the lacustrine facies filling the dissolution cavities provide evidence for the re-submersion of the buildups and greater hydrodynamics. Donsimoni (1975) proposed that this tabular structure was induced by the formation of a natural dam and compares them to the travertines of Afghanistan described by Lang (1984). However, the Chadrat facies do not show any evidence of hydrothermal activity frequently described for the travertines (Della Porta, 2015). In Jussat, the shallow domain is colonized by abundant caddisfly pupal cases and *Cladophorites* that constitute the nucleation point for carbonate buildups. They preferentially developed in the wave-dominated littoral area (Hugueney *et al.*, 1990; Freytet, 1998; Leggitt *et al.*, 2007). The dome, cone and coalescent columns, the macrofabrics displaying an important synoptic relief, result from an increasing accommodation. In the Jussat area, the maximum height of the buildups (ca. 4 m) suggests that the water depth was usually lower than 5 m. The buildups from the central Limagne Basin are systematically smaller than those observed in the northern Limagne Basin, which can reach 10 m in height (Wattinne *et al.*, 2003; Roche *et al.*, 2018). The palustrine facies, mainly represented by marly and muddy facies with subaerial exposures, desiccation cracks, chip levels and karstification, indicate a low-energy platform along a gentle lake margin (Alonso-Zarza and Wright, 2010).

6.2 Sedimentary cycles

As proposed in Roche *et al.* (2018), the different outcrops show a high frequency, repetitive succession (cycle) of lacustrine to palustrine facies. Figure 16 summarizes the main characteristics of the cycles with a comparison to the one proposed for the northern Limagne Basin (Créchy). The base of the cycles corresponds to a lacustrine unit comprising well-developed microbial deposits. This unit is poorly developed in the Grand Gandaillat and Chadrat outcrops while it is thicker in the Jussat and Créchy outcrops. A palustrine unit overlies the lacustrine one. These littoral to continental facies were relatively thick during the Chattian and the palustrine part

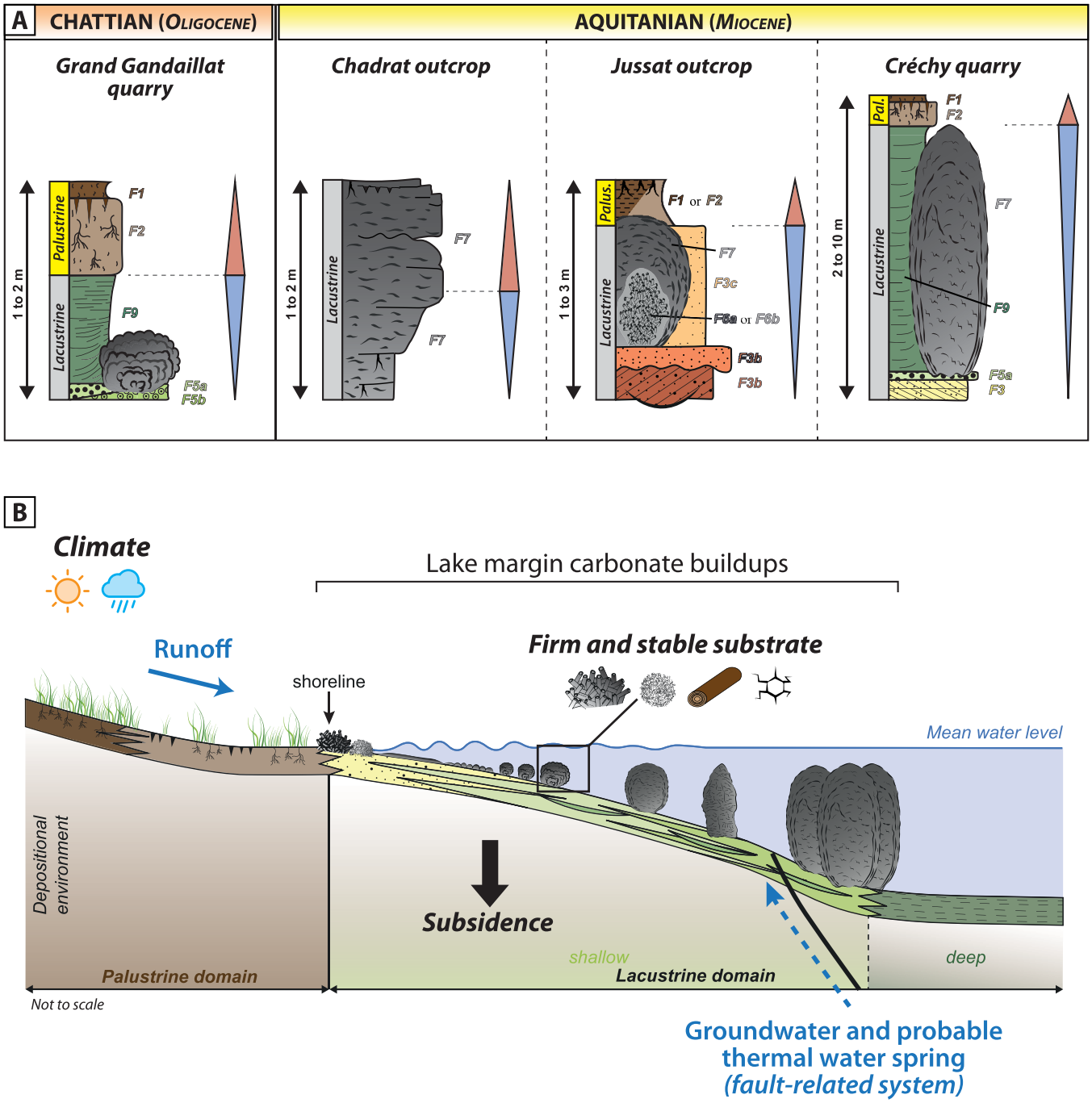

Fig. 16. Lacustrine/palustrine ratio for the Chattian and Aquitanian cycles. Each cycle is organized in five steps; Chattian cycles (Grand Gandaillat quarry) with a low carbonate *versus* clastic ratio with thin microbial-rich buildups, presence of pure illite and intense desiccation cracks in the palustrine deposits; Aquitanian cycles (Chadrat and Jussat outcrops and Créchy quarry) with a high carbonate *versus* siliciclastic ratio with thick microbial and metazoan buildups (see Fig. 5 for caption). The main characteristics of the steps are detailed.

of the cycle became thinner during the Aquitanian, or was even absent or not preserved at all in Jussat and Chadrat outcrops. Each cycle is characterized by a first deepening trend followed by a shallowing-upward one, which indicates environmental changes related to high-frequency fluctuations in the lake level and high-to-low hydrodynamic conditions. In Grand Gandaillat, the cycles are symmetrical with a relative equal thickness of the lacustrine and palustrine deposits (Fig. 16). The same pattern has already been described in the literature for the Chattian deposits of the Créchy quarry (Wattinne 2004; Wattinne *et al.*, 2018). On the contrary, the cycles evidenced in Jussat and Créchy are asymmetrical, with thicker lacustrine deposits (and thus shoreline expansion) than the palustrine ones (Fig. 16). Both symmetrical and asymmetrical cycles

follow a five-step model that has already been discussed in Roche *et al.* (2018). However, the thickness of the Aquitanian cycles differs between the northern and southern part of the Limagne Basin. In the central Limagne Basin (Jussat), the cycles are thinner than the ones described in the northern Limagne Basin (1 to 3 m *vs.* 2 to 10 m) and, locally, present medium to coarse clastic deposits (Fig. 16). Steps 1 to 3 develop within a context of increasing accommodation while steps 4 and 5 record a decreasing accommodation. Step 1 initiates over either a basal erosion surface or an emersion one. The facies are made of sands, floatstones rich in wood fragments or peloid/ooid-oncoid grainstones and are interpreted as the shoreline domain. Step 2a is characterized by the initiation and development of the first buildups, with a low synoptic relief in shallow water. They are mainly composed of caddisfly pupal case accumulations or *Cladophorites* bushes. These first-built structures can be encrusted by microbial-rich layers forming macrostructures with variable morphologies (Step 2b) and embedded by carbonate sands (F4; Step 3) or sandstones (F3; Step 3). When located in the fan delta environment, the structures formed by caddisfly pupal case accumulations or *Cladophorites* bushes were poorly encrusted by microbialites. Steps 2 and 3 depict the maximum lake level, and thus lake expansion. In the central Limagne Basin, the absence of deep lacustrine marls, the progradation of the fan delta and the thinner cycles provide evidence for shallow conditions with low accommodation. The cycle ends with the installation of the palustrine facies (Steps 4 and 5). The palustrine deposits represent episodes of reduced accommodation (Alonso-Zarza and Wright, 2010). Each cycle is limited by widely traceable surfaces that are marked by desiccation cracks, dissolution cavities and root traces. Throughout the Chattian and Aquitanian successions, the restoration of full lacustrine conditions requires a positive water budget. Lake-level fluctuations could have been induced by various mechanisms, such as climate and tectonics (Madsen *et al.*, 2001).

6.3 Factors controlling the development of fossil buildups

Each visited outcrop offers an opportunity to discuss the main controlling factor involved in the formation and development of the metazoan and microbial-rich buildups during the Chattian and Aquitanian. Even though each of these outcrops was involved in the global understanding of sedimentation in the Limagne Basin, the specificities of each outcrop are highlighted in the following section.

6.3.1 The carbonate factory and the biotic/abiotic influence on microbial-rich deposits

The dominant carbonate factory of the lacustrine Limagne deposits is driven by both (1) abiotic and (2) biotically-induced processes. These processes are two of the dominant carbonate factories proposed by Schlager (2000) in aquatic realms (the third is the biotically-controlled factory). It corresponds to the M-factory characterized by the microbial-mediated (*e.g.* bacteria including cyanobacteria) precipitation of mud (Schlager, 2000, 2003). The most prominent features of this factory are microbial mats, which usually contain several microbial genera and species from various key metabolic groups (*e.g.* cyanobacteria, anoxygenic phototrophs, sulfate reducers; Visscher and Stolz, 2005; Baumgartner *et al.*, 2009), and their organic EPS (extracellular polymeric substances) matrix steering the different organo-mineralization processes (Dupraz *et al.*, 2009). These different organo-mineralization processes may produce diverse microbialites through a variety of *in situ* carbonate precipitating and lithification processes potentially present in various aquatic environments (Dupraz *et al.*, 2009; Della Porta, 2015).

The filamentous microfabrics of the bioconstructions of the Limagne Basin are particularly well preserved in Chadrat, where they show diverse and clearly identifiable morphologies despite the overprint of diagenesis, pedogenesis and karstification (Figs. 5 and 6). Freytet (2000) attributes their origin to green algae, however, he specifies that other frequent microorganisms have similar morphologies such as cyanobacteria, chlorophyceae, xanthophyceae (unicellular algae), phaeophyceae (brown algae) and rhodophyceae. Since the work of Freytet (2000), similar filamentous structures have been reported from many continental environments: in lakes (*e.g.* Great Salt lake, USA, Vennin *et al.*, 2019; Mono Lake, USA, Guo and Chafetz, 2012; Brasier *et al.*, 2018; Pyramid Lake, USA, Arp *et al.*, 1999), hydrothermal vents (*e.g.* Italy, Della Porta, 2015; Bolivia, Bougeault *et al.*, 2019), and in rivers (*e.g.* Japan, Kano *et al.*, 2003; Slovakia and Poland, Gradziński, 2010; Spain, Arenas *et al.*, 2014; Roche *et al.*, 2019). The filamentous structures are identified as either molds or the remains of cyanobacteria (*e.g.* Freytet and Verrecchia, 1998; Arp *et al.*, 1999; Brasier *et al.*, 2018; Vennin *et al.*, 2019). These structures present some similarities with the "shrub", formed by in-situ upward growth from a lake substrate, descripted in the Aptian lacustrine deposits of Brazil. Many authors (*e.g.* Wright and Barnett, 2015; Herlinger *et al.*, 2017; Souza *et al.*, 2018; Lima and De Ros, 2019; Farias *et al.*, 2019; Gomes *et al.*, 2020) have considered these deposits as abiotic carbonate since they recognize some morphometric similarities with travertine deposits. Wright and Barnett (2015), Lima and De Ros (2019) and Wright (2021) assumed that the formation of shrubs is the combined result of changes in the lake water chemistry related to climate, abiotic precipitation resulting from CO_2 loss by evaporation, magmatic CO_2 input and hydrothermal activity. Although these authors admit that microbial mats were present in the lakes, they consider that the extreme alkalinity conditions reduced the level of metabolic activity to a point where biotic processes were minimized and thus the abiotic precipitation of carbonates predominated. It should be noted that microbial metabolisms notably alter the alkalinity and highly alkaline environments may support microbial mat development (Boomer *et al.*, 2009; Dupraz *et al.*, 2013). Indeed, alternative hypotheses suggest that biological factors triggered the initiation of the shrubs (Chafetz and Folk, 1984; Chafetz *et al.*, 2018; Ceraldi and Green, 2017). The association with early sparitic precipitation indicates a possible combination of biotic and abiotic carbonate precipitation processes. More specifically, early diagenetic imprints are easy to recognize in microfabrics if the microbial activity is partly preserved as mold or filament. A secondary diagenetic mineralization superimposed on the primary lamination makes it difficult to determine the biotic *vs.* abiotic origin for the development of

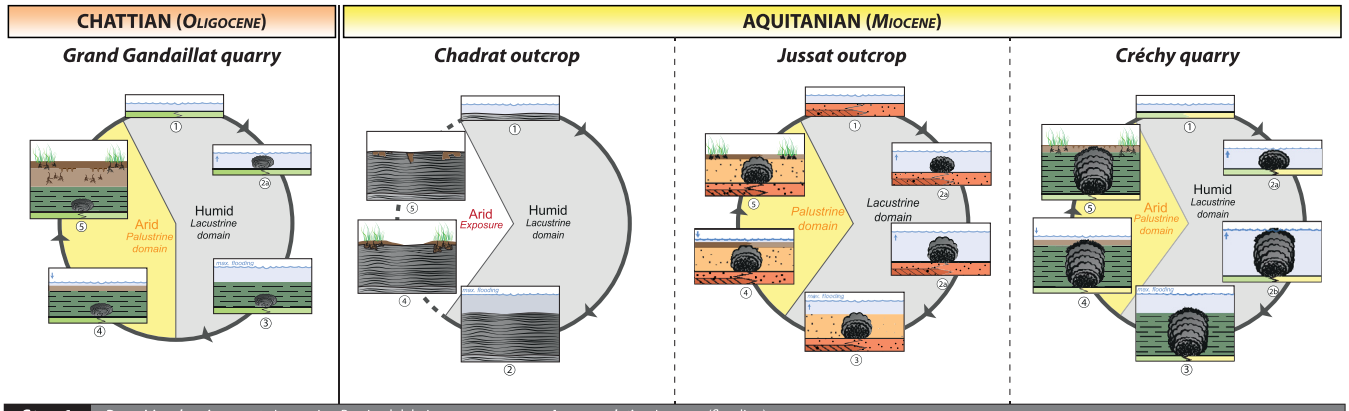

Step 1 *Depositional environments*: Lacustrine-Proximal deltaic *Accommodation*: Increase (flooding) Cm to pluri-dm thick microconglomeratic sands (F3a) and/or cm to dm thick carbonate carbonated sands (cortoid-F3b/ooid-F3c/peloid-F3d) or microbial-rich builups (F7)			
Erode palustrine deposits (F1 or F2) and sometimes rest directly on emersion surface		Rest either on sandstones or directly on the erosion surface of the palustrine deposits	
Step 2a *Depositional environments*: Shallow lacustrine-Deltaic *Accommodation*: Increase (short-term floodings alternating with subaerial episodes)			
Microbial-rich buildups (flat and cauliflower; F7)	Microbial-rich buildups and rare caddisfly (F6a) and microbial-rich buildups (biostrome with flat and columnar laminated mesofabrics)	Diversified mixed caddisfly (F6a) or *Cladophorites* (F6b) and microbial-rich buildups (Flat and cauliflower macrofabrics) ; clusters of caddisfly pupal cases or bushes of *Cladophorites*	Diversified mixed caddisfly (F6a) and microbial-rich buildups (flat and cauliflower; F7)
Step 2b *Depositional environments*: Shallow to deep lacustrine *Accommodation*: Maximum flooding			
		Diversified buildups as domes, cones and coalescent macrofabrics (F7 and F8) with a core made of cauliflower or microbial-rich (Step 2a); caddisfly pupal case accumulations on top of some buildps	
Step 3 *Depositional environments*: Deep to shallow lacustrine *Accommodation*: Maximum flooding			
Varve couplets composed of mm to cm-thick organic matter-rich marls alternating with carbonate layers (F9); Embed and cover buildups		Pluri-dm to-m-thick sands (F3b and F3c), which embed and cover only small-size buildups and organic matter-rich marls (only high accommodation)	Varve couplets composed of mm to cm-thick organic matter-rich marls alternating with carbonate layers (F9); Onlap the wall of the buildups
Step 4 *Depositional environments*: Palustrine *Accommodation*: Decrease Development of palustrine deposits (F1 and F2), progressive transition to carbonate beds with paleosols and traces of emersion (desiccation and root traces)			
Carbonate beds < 1m-thick developed on top of marls	Root traces are frequently observed on top of the microbial-rich buildups or frequently eroded.	Carbonate beds < 0,5m-thick developed on top of small-size buildups or lateraly to the emersion surface observed on top of the buildups	
Step 5 *Depositional environments*: Palustrine *Accommodation*: Emersion			
Pure illite/argilaceous layers with root traces	Emersion surface and karst	Pure illite/argilaceous layers with root traces	

Fig. 17. (A) Elementary sedimentary successions; Symmetric Chattian sedimentary succession (Grand Gandaillat) where buildups only correspond to flat and cauliflower macrofabrics and asymmetric Aquitanian sedimentary successions (Chadrat, Jussat and Créchy), thinner in Chadrat and thicker in Créchy, respectively. The buildups are diversified and composed of all the macrofabrics. (B) Main controlling factors of the Limagne Basin sedimentation.

the cemented structures in the buildups. De Boever *et al.* (2017) proposed an overview and a short, non-exhaustive list of petrographic characters towards the recognition of primary textures in non-marine carbonates, but additional geochemical and microbiological analyses are necessary. They concluded that the presence and activity of microorganisms and organic matter seems to have a profound impact, not only on the precipitation of carbonates, but also on the micro-scale localization of early diagenetic processes (replacement) that rapidly transform the primary microfabrics. *Broutinella arvernensis* described in the Limagne Basin is considered as a combined association of biotic (filamentous bacterial development) and abiotic (cements) processes, but could also result from early diagenesis. The lateral variation from filamentous to cements, the presence of cements mainly toward the edges of the buildups and the repetitive succession of filamentous-rich and cement-rich layers point to high-frequency alternating dry and wet episodes associated with change in physico-chemical conditions (Bougeault *et al.*, 2019). Carbonate precipitation depends on multiple factors (intrinsic, extrinsic and environmental) and results from a continuum of physico-chemical and microbial processes that are biologically induced or influenced (Dupraz *et al.*, 2009). Consequently, the analysis and identification of the contribution of each of these factors to precipitation are difficult, even more so in the fossil record (*e.g.* Brasier *et al.*, 2018).

The buildup diversity and composition seemed to have been modified between the Chattian and Aquitanian, and usually evidenced environmental changes (Fig. 2). The low diversity and predominance of *Broutinella arvernensis* in the Chattian buildups of Grand Gandaillat is considered as resulting from peculiar chemical conditions and a thermal stratification of the lake, favoring shallow anoxic conditions (Wright and Barnett, 2015; Bouton *et al.*, 2016; Roche *et al.*, 2018). In addition, the small size and scarcity of the buildups formed at the Oligo-Miocene transition may be related to brackish conditions, as suggested by the faunal association (*i.e.* gastropods and ostracods; Hugueney *et al.*, 2003). In contrast, the Aquitanian buildups became dominated by larger and more diversified structures, mainly composed of micro-

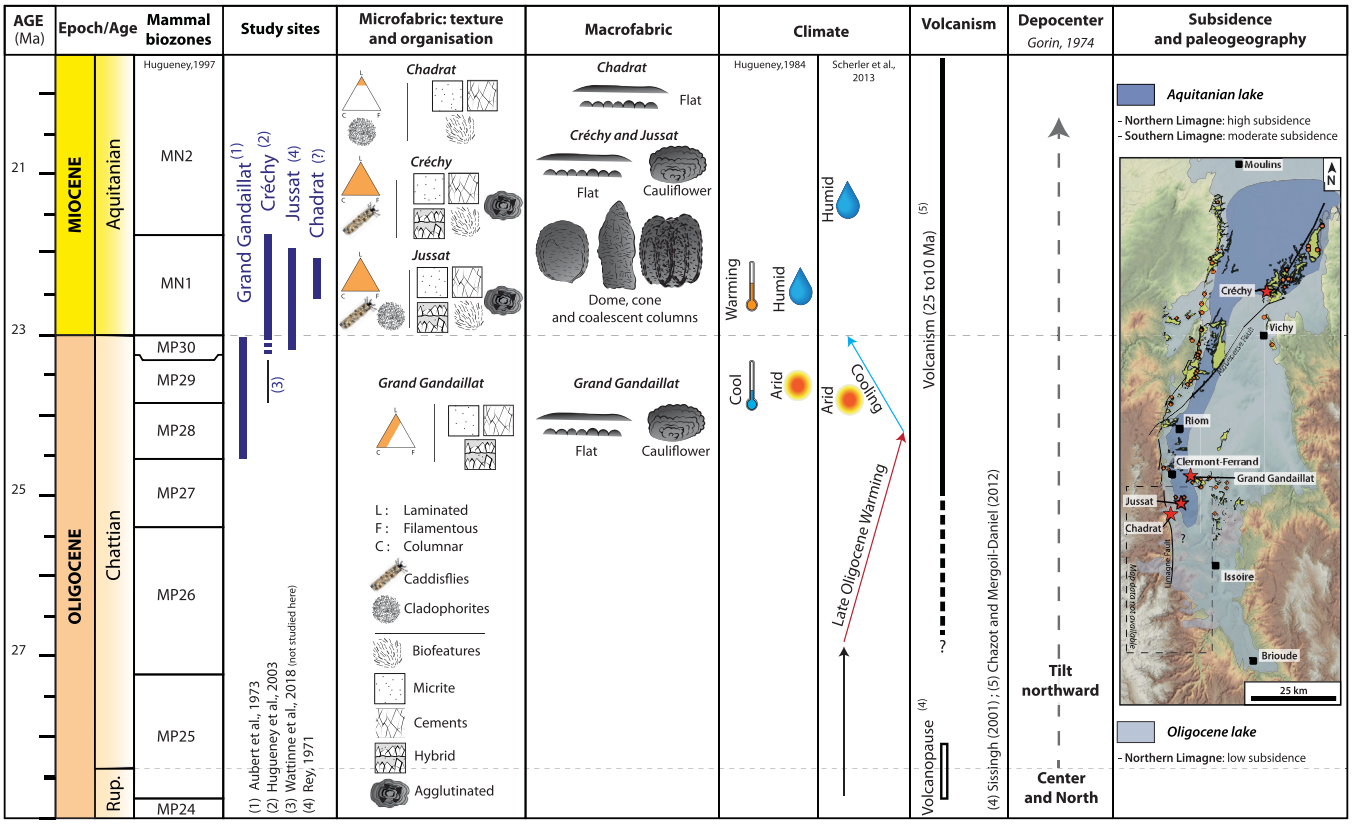

Fig. 18. Summary of the stratigraphy and morphology of the buildups as well as the main controlling factors (climatic, tectonic, volcanic events and substrate) affecting the Limagne Basin since the Early Oligocene (the age are deduced from the geochronology and biostratigraphy based on palynology and mammalogy data; Hugueney, 1997; see Fig. 5 for caption).

bialites and caddisflies. In Jussat, the buildups differ from those of Créchy (described in Roche *et al.*, 2018) by the presence of *Cladophorites*, another contributor to the initial development of buildups. *Cladophorites* were never found in association with caddisfly pupal case accumulations, as they were probably removed by grazing organisms (Garrett, 1970; Javor and Castenholz, 1984; Tinsley *et al.*, 2016). Consequently, the massive presence of caddisfly pupal cases may have prevented the development and/or preservation of *Cladophorites*. The local preservation of *Cladophorites* may also indicate a change in the physico-chemical conditions of the lake, as they tolerate variations in salinity (fresh to brackish water; Riding, 1979; Arp, 1995).

6.3.2 Contrasting buildup composition, size and distribution through time

During the Chattian and Aquitanian ages, the central Limagne Basin hosted a perennial lake system. However, climatic, tectonic, volcanic and other local controls affected its sedimentary dynamics (Figs. 17 and 18), resulting in spatial and temporal differences in the (i) cycle organization, (ii) composition of the sediments, (iii) distribution and (iv) development (in the case of buildups).

(i) The sedimentary record of the Jussat, Chadrat and Grand Gandaillat outcrops, and more generally the whole Limagne Basin, is organized in cycles (see Sect. 6.2), a feature commonly encountered in palustrine-lacustrine environments. While the interpretation of the cycles is frequently related to climatic fluctuations in open lake areas (*e.g.* Bohacs *et al.*, 2000), short-term subsidence episodes cannot be ruled out, reflecting the influence of tectonic factors (Alonso-Zarza and Wright, 2010). In the Limagne Basin, the Oligo-Miocene sedimentary cycles usually comprise a lacustrine part and a palustrine part. However, a difference between the Aquitanian and Chattian cycles has been evidenced by Roche *et al.* (2018): the Aquitanian cycles are thicker and considered as asymmetrical (the lacustrine parts are more developed than the palustrine ones); on the contrary, the Chattian cycles are thinner and symmetrical. The composition and size of the buildups also differ between the two time intervals: the Chattian buildups are exclusively microbial and only a few centimeters high, whereas the Aquitanian ones may reach several meters in height and are composed of both microbes and metazoans (caddisfly pupal cases and *Cladophorites*, mainly). Climatic, tectonic, volcanic and local parameters were proposed as the main control on the deposition of buildups and their organization in each different cycle (Wattinne *et al.*, 2003; Roche *et al.*, 2018). However, the change in the cycle symmetry observed at the Oligo-Miocene transition can instead be attributed to a long-term climatic control, with thin and symmetrical cycles during the drier Chattian and thick and asymmetrical ones during the wetter Aquitanian.

(ii) The Jussat outcrop differs from the other studied sites by the presence of significant siliciclastic deposits (Fig. 17). These clastic accumulations, and thus inputs, may have both a climatic and tectonic origin (Platt, 1989; Platt and Wright, 1991; Kreuser, 1995). An increase in precipitation will induce an increase in surface runoff which, by promoting weathering and transport, will allow the deposition of siliciclastic sediments (Platt, 1989; Carroll and Bohacs, 1999; Bohacs *et al.*, 2000; De Wet *et al.*, 2015). The significant clastic accumulations recorded in Jussat are then consistent with the humid climate proposed for the Aquitanian (Chateauneuf, 1972; Hugueney, 1984; Scherler *et al.*, 2013). In contrast, the dry climate proposed for the Chattian (Gorin, 1975; Zachos, 2001) is consistent with the low content of clastic sediments preserved in Grand Gandaillat.

The composition, organization and geometry of the sediments in the Jussat outcrop suggest a deltaic depositional environment, emplaced at the mouth of a river. The clastic contributions within a lake can be localized close to reliefs (Platt and Wright, 1991), and reflect a specific paleogeographical position as deltas are shore related features (Schuster and Nutz, 2018). Some local factors may also modify the input and/or distribution of clastic sediments, such as the vegetation. Stabilization of the banks by the vegetation may facilitate the trapping of siliciclatic deposits (Dunagan and Driese, 1999; Schnurrenberger *et al.*, 2003).

(iii) Lacustrine systems can be deeply affected by climatic and tectonic changes, which modify the hydrological conditions, the basin morphography and the sedimentary dynamics. At the Chattian/Aquitanian transition, a long-term climatic change toward wetter conditions coupled to a regional uplift tilting northward in the central Limagne Basin have resulted in a modification of the distribution and thickness of the sediments (Fig. 18; Roche *et al.*, 2018). Carbonates, especially microbial, constitute prime tools to investigate environmental and paleogeographical variations (through space and time) as they are very sensitive to changes. The spatial distribution of the buildups and sedimentary structures may constitute accurate proxies to reconstruct the water level fluctuations through time. In the Limagne Basin, most of these fluctuations can be explained by climatic variations (*e.g.* Chateauneuf, 1972; Hugueney, 1984; Roche *et al.*, 2018). However the peculiar straight distribution of the buildups along the regional faults raises the question of whether tectonics may be an additional driver for the development and distribution of the buildups (Fig. 2). Faults can produce structural microtopographic highs and thus impact the development and distribution of buildups from a local to regional scale (Bouton *et al.*, 2016; Gomes *et al.*, 2020). Given that they allow the circulation of groundwater rich in ions (Ca^{2+}; HCO_3^-), fault systems also promote the mineralization of microbial buildups (Arenas *et al.*, 2015). This last explanation is commonly proposed to justify the alignment of microbialites along faults (*e.g.* Lake Van in Turkey; Kempe *et al.*, 1991; Cukur *et al.*, 2015; Mono and Searles Lake in the USA; Rieger 1992; Guo and Chafetz, 2012; Great Salt Lake, USA; Bouton *et al.*, 2016; Janecke and Evans, 2016, 2017; Early Cretaceous, Brazil; Gomes *et al.*, 2020). Currently, several studies provide evidence for a significant degassing of CO_2 linked to faults in the Limagne Basin (*e.g.*De Lary *et al.*, 2016; Bräuer *et al.*, 2017; Duwiquet *et al.*, 2019). Isotopic analyses have shown that the CO_2 has a mantle signature and is found in association with listric faults anchoring in the lithosphere, serving as drains for hydrothermal flows (*e.g.* Bräuer *et al.*, 2017; Ars *et al.*, 2019; Duwiquet *et al.*, 2019). A hydrothermal activity, similar to the one recorded currently, is supposed to have occurred at the end of the Eocene, in association with the rift magmatism. Indeed, many modern rift systems (*e.g.* East African rifts, Coussement *et al.*, 1994; Lee *et al.*, 2016; Wilks *et al.*, 2017; the New Zealand Rift, Rowland and Sibson, 2004), show that extensive magmatism is accompanied by hydrothermal activity, which can directly influence the chemistry of the lake (Renaut *et al.*, 2017). The impact of hydrothermalism on the sedimentation of the Limagne Basin was already suggested by the distribution of gastropods (Valvatidae) only along the Aigueperse fault during the Aquitanian (Rey, 1964; Wattinne, 2004; Fig. 2).

(iv) The magmatic activity of the region also seems to have deeply affected the bio-physico-chemical conditions of the lake, and thus the development of the microbial buildups. For example, Bertrand-Sarfati *et al.* (1966) proposed that the development of caddisfly pupal cases was linked to hydrothermal activity. However, the effects of the magmatic framework are not limited to the hydrothermal flow; some phreato-magmatic events and associated deposits may have impacted the sedimentation. A phreato-magmatic activity that persisted from the Chattian to the Early Aquitanian has been recorded in the Grand Gandaillat area (Fig. 13; Goër de Hervé, 2000; Michon, 2000; Chazot and Mergoil-Daniel, 2012). A phreato-magmatic activity that persisted from the Chattian up to the Early Aquitanian has been recorded in the Grand Gandaillat area (Fig. 18; Goër de Hervé, 2000; Michon, 2000; Chazot and Mergoil-Daniel, 2012). The influence of volcanism on subaerial and lacustrine deposits in a rift setting has been extensively discussed (Cerling, 1994; Wright and Barnett, 2015; Szatmari and Milani, 2016) and contributes to the changes in the alkaline conditions and/or the modification of magnesium, calcium and silica concentrations in lakes (Cerling, 1994; Armienta *et al.*, 2008) in lakes. In the Grand Gandaillat outcrop (Chattian), the peperites are clearly syn-lithication to post-lithification since dykes and peperitic sills intersect the sedimentation of the lake. In contrast, the peperites seem to be located topographically below the lacustrine deposits in Jussat (Aquitanian). However, the vegetation cover, the lack of dating and the presence of a fault (as proposed by Morange *et al.*, 1971) in this outcrop mean that it is not possible to propose a robust correlation or chronology between the deposition of the peperites and the lacustrine sedimentation. By increasing the local heat gradient, the peperites could also support the local maturation of the organic matter present in the sediments, as observed in the Grand Gandaillat quarry and in Puy de la Poix. Since they are rich in silicium, the dissolution of these phreatomagmatic rocks may be responsible for the occurrence of late silica-rich diagenetic features (Lussatite; Mallard, 1890).

The development of the microbial buildups may have also been controlled by the substrate (Fig. 17; Della Porta, 2015; Bouton *et al.*, 2016). Recently, Roche *et al.* (2019) and Vennin *et al.* (2019) discuss the role of substrate on the mineralization potential and distribution of continental microbial deposits and tufa. The presence of hard substrate, by its stability and the limited disturbance, enhances the development and preserva-

tion of microbial mats (by limiting the effects of erosion) and thus favors lithification (Della Porta, 2015; Bouton *et al.*, 2016; Roche *et al.*, 2019; Vennin *et al.*, 2019). In the Limagne Basin, the largest microbial buildups (domes, cones, columns and coalescing macrofabrics) develop exclusively on caddisfly pupal case accumulations and *Cladophorites*. Therefore, biotic components appear to be favorable substrates for the development of microbialites and, in addition, to determine the distribution of the buildups. The microbialites themselves, due to their rapid mineralization and lithification, constitute a favorable substrate for further buildup formation as observed in Chadrat. As underlined by the molding imprints of plant structures at the base of the microbialites, wood fragments also represent an ideal substrate for the development of microbial deposits. Furthermore, as observed in Jussat, the buildups preferentially developed on coarse substrates; only a few rare examples of planar macrofabrics were reported on fine substrates. These observations support the hypothesis that the formation of microbialites is controlled by the presence of firm and stable substrates, including those from a biotic origin (*e.g.* Casanova, 1994; Dromart *et al.*, 1994; Winsborough *et al.*, 1994; Ginsburg and Planavsky, 2008; Saint Martin and Saint Martin, 2016).

6.4 The contribution of modern microbial deposits to understanding the mineralization and preservation processes.

One of the peculiarities of the Limagne Basin is that it hosts fossil (Cenozoic) microbial deposits and modern microbial mats. Although modern occurrences cannot be considered as exact analogues to the Chattian and Aquitanian buildups, understanding their development and biogeochemical cycling (including carbonate precipitation), may improve our ability to decipher the processes that lead to the formation of fossil microbialites. Modern microbial mats can be found in two spring systems: Sainte-Marguerite and the Puy de la Poix area. The first system comprises a thermal spring, and the second system is associated upwelling of bitumen- and sulfate-rich water. Since the physico-chemical conditions strongly differ between the two sites, each is unique in terms of the dominant microbial communities and associated biological mineralization. Despite the fact that the Sainte Marguerite bio-hydrogeosystem can be considered of endogenic travertine origin (Pentecost, 2005; Crossey *et al.*, 2009), in addition to abiotic processes, biotic activity has been proposed in order to explain the formation of the carbonates. Changes in the mineralization intensities may be explained by the specific physico-chemical conditions (*e.g.* calcite saturation index (SI_{calc}) and the partial pressure of CO_2 (pCO_2) and close proximity of the cyanobacterial biofilm and carbonate precipitates. Preliminary observations at Sainte Marguerite suggest that the microbial mats are involved in microbially-mediated carbonate precipitation (Fig. 15). The production of O_2 bubbles suggests high rates of oxygenic photosynthesis; the white sheen at the water interface is indicative of rapid sulfur cycling, similar to what has been observed in hypersaline and marine microbial mats forming microbialites (Dupraz and Visscher, 2005; Dupraz *et al.*, 2011). It has been suggested that microbes mediate the formation of hydrous iron oxides and carbonates in modern low-temperature CO_2-rich spring waters in Cézallier (Casanova *et al.*, 1999). The microbial mats of Sainte Marguerite resemble the mats that thrive in Yellowstone National Park (USA; Fouke, 2011) or those present near the hydrothermal field associated with the Taupo Fault Zone (New Zealand; Brock and Brock 1971). The microbial coating of various surfaces by cyanobacterial mats is sometimes referred to as tufa-travertine (Freytet and Plet, 1996) and the roles of microbial mats and cyanobacteria in travertine deposits have been studied extensively in Mammoth Springs (Castenholz 1977; Fouke *et al.*, 2000; Fouke, 2011). The preliminary results obtained from SEM investigations of microbial mats and associated carbonate precipitates have highlighted the role of the biotic components, especially microorganisms and EPS (Fig. 15) in mineral precipitation. The micro-peloids (Fig. 15E) found in the carbonate deposits of Sainte Marguerite are similar to the ones observed by Payandi-Rolland *et al.* (2019) in the Merantaise River and by Payandi-Rolland *et al.* (2019) in laboratory experiments. The formation of micro-peloids is likely mainly related to the activity of filamentous cyanobacteria and possibly diatoms although the entire microbial mat community ultimately determines the net precipitation result (Dupraz and Visscher, 2005; Dupraz *et al.*, 2009. The presence of nanostructures (nanospheres, and agglutinated triangular polyhedra) argues for a biologic role on the mineralization (Folk, 1999; Manzo *et al.*, 2012; Perri *et al.*, 2012; Roche *et al.*, 2019). Concerning the coated bubbles, similar microstructures were described in travertines from Yellowstone (USA; Fouke *et al.*, 2000) and Saturnia (Italy; Ronchi and Cruciani, 2015). The complex structures of the coated bubbles and their association with EPS observed at the water-air interface along the stream may suggest a biotic influence on the observed mineralization.

In closing, it should be noted that presence of cyanobacteria does not necessarily imply that there is oxygenic photosynthesis as observed in Puy de la Poix. The metabolism of the phototrophs is very diverse and the capacity to perform anoxygenic photosynthesis has been demonstrated in cyanobacteria as well as many in anoxyphototrophs. Thus, the presence of a fossil microbial mat (microbialites) does not imply the presence of oxygen. Furthermore, it should be noted that the layering in microbial mats is not the same as the lamination in microbialites: an entire microbial mat was found to form one layer in the open marine Bahamian and Cuban stromatolites (Reid *et al.*, 2000; Pace *et al.*, 2018). Near the surface, cyanobacteria produce EPS and increase the alkalinity through oxygenic photosynthesis during the daytime (Dupraz and Visscher, 2005). Deeper in the mat, the rapid consumption of oxygen through aerobic respiration (using O_2 as an electron acceptor) leads to the formation of an anoxic environment, in which anaerobic metabolisms are then responsible for the oxidation of the remaining organic matter using other terminal electron acceptors for respiration (*e.g.* SO_4^{2-}, NO_3^-, Fe^{3+}). This general notion has evolved further when it was demonstrated that sulfate-reducing bacteria (SRB) are metabolically very active near the surface of the mat in the photosynthetically active, oxic zone (see Visscher *et al.*, 1991; Baumgartner *et al.*, 2006 for a review; Pace *et al.*, 2016). In Sainte Marguerite, sulfate is abundant in the water, and then SRB could play an important role in microbialite formation as they usually increase the carbonate alkalinity and remove

sulfate which inhibits carbonate precipitation (Vasconcelos and McKenzie, 1997; Visscher *et al.*, 2000; Dupraz *et al.*, 2009). The study of microstructures and their relation with biological components facilitate a better understanding of a biotic *vs.* abiotic origin of the tufa microbialites. Even if some authors proposed a purely physico-chemical role in the shape of crystals (Pedley, 1992; Reid *et al.*, 2000), the role of microorganisms has been also recognized (Dupraz *et al.*, 2009; Della Porta, 2015). The supersaturation of the water with respect to calcite is a fundamental condition that is required to trigger mineralization in lacustrine settings. Even if the abiotic processes govern induction of mineralization and carbonate precipitation in the fan-shape delta of Sainte Marguerite, biological factors played a critical role in the mineralization processes. These results are encouraging and may enable a better understanding of the microbially-induced or -influence carbonate precipitation in the fossil record.

7 Conclusion

This publication results from a fieldtrip organized in the Limagne Basin as part of the *Microbialites: formation, evolution and diagenesis (M-Fed)* meeting (October 2019). The objective of this paper is to assess the diversity of modern and fossil (Chattian to Aquitanian) microbial sediments and structures through a regional sedimentological and stratigraphic study. Investigations carried out in various Oligo-Miocene outcrops found in the central Limagne Basin demonstrate the potential impact of the climate, tectonic and volcanism in the sedimentary dynamics of the basin, especially carbonate buildups and microbialites. The microbial and metazoan buildups from the Limagne display five different macrofabrics (flats, cauliflowers, domes, cones and columns) and four main microfabrics (laminae, columns, filaments and their association with other biotic components). Three main depositional models were proposed from the different outcrops and show the spatial and temporal evolution of the Chattian and Aquitanian buildups.

All of the fossil outcrops visited record several lacustrine/palustrine cycles. While the symmetrical Chattian cycles result from long-term dry climatic conditions, the Aquitanian counterparts provide evidence for wetter conditions. The difference in the thickness and non-random distribution of the microbial and metazoan buildups along the faults are related to the tectonic framework. In Jussat, the presence of thinner cycles during the Aquitanian (in comparison to those recorded in the northern Limagne Basin) and a fan delta are consistent with the hypothesis of a regional uplift tilting northward in the central Limagne Basin. The Grand Gandaillat and Puy de la Poix outcrops are characterized by bitumen seep resulting from the transformation of the organic matter deposited in the deep lacustrine marls. The modern microbial communities of Sainte Marguerite can be compared with those developed in association with modern endogenic travertine. The microbial deposits observed in the Limagne setting show that carbonate production continues today in connection with fluid circulation within the basin. The specific mineralization processes described in relation with the microbial mats provide in-depth insights into understanding fossil microbial-induced precipitation of the Oligo-Miocene lacustrine carbonates.

Supplementary Material

Figure S1. SEM images of cut and polished coated bubble: (A) cross-section of a cut bubble. The B-F areas are located as white rectangles; (B) needle-like $CaCO_3$ crystals in external layers of the coated bubble's wall; (C) rosette-shaped $CaCO_3$ crystals in the external layers of the coated bubble's wall; (D) spherical radial needle crystals of $CaCO_3$ forming the inner layers of the coated bubble; (E, F) hemispherical radial needle crystals of $CaCO_3$ in the internal part of the bubble; (G) schematic cross-section of the cut bubble with the location of image A.
Figure S2. FTIR spectra of coated bubble (source: Rruff database): (A) aragonite with characteristic peaks of intensity at 699, 712, 855, 1082 and 1446 cm^{-1}; (B) calcite with characteristic peaks at 712, 871, 1165, 1399 and 1796 cm^{-1}. Additional peaks correspond to the LR-white resin.
Table S1. Description of the facies and their depositional environments.

The Supplementary Material is available at http://www.bsgf.fr/10.1051/bsgf/2021030/olm.

Acknowledgements. The authors would like to thank Elias Samankassou and an anonymous reviewer whose work has helped to improve the manuscript. The authors would like to thank Total E&P (FR00008732) for funding the project and this study is a contribution from Total R&D (supervisor, E. Poli). This work is a contribution from the SEDS team at the Biogéosciences Laboratory (University of Bourgogne/Franche-Comté, France) and the I-site project UB18016-BGS-IS. We are very grateful to Lionel Weitz and the Vicat Society for providing access to the quarries. We are also grateful to all of the people who participated in the fieldtrip in October 2019 for their helpful discussions (Afroz Munira, Barreiros Heitor, Bielski Paul, Bougeault Cédric, Boussagol Pierre, Bouton Anthony, Brito Marlisa, Bundeleva Irina, Decraene Marie-Noëlle, Des Marais David, Durlet Christophe, Gallois Arnaud, Gaucher Eric C., Gérard Emmanuelle, Ghosh Parthasarathi, Lalonde Stefan, Martín-Pérez Andrea, Muller Elodie, Patry Laureline, Portier Eric, Ragazzo Alfonso, Ramsay Brittnay, Roche Adeline, Sansjofre Pierre, Vennin Emmanuelle, Visscher Pieter and Wilmeth Dylan). The organizers of the field trip gratefully acknowledge the Arkose Association for their support on the field. We also thank Pascal Taubaty for preparing the thin sections. Authors are thanking Emilie Steimetz (Bourgogne Franche Comté University, Platform Gismo) for SEM acquisition and Jonathan Edwards (ESRI France) for his help with GIS.

References

Adiya T, Johnson CL, Loewen MA, Ritterbush KA, Constenius KN, Dinter CM. 2017. Microbial-caddisfly bioherm association from the Lower Cretaceous Shinekhudag Formation, Mongolia: Earliest record of plant armoring in fossil caddisfly cases. *PLoS ONE* 12: e0188194–e0188194.

Alonso-Zarza AM, Wright VP. 2010. Chapter 5: Calcretes. In: Alonso-Zarza AM, Tanner LH, eds. *Developments in Sedimentology*, 61. Elsevier, pp. 225–267.

Arenas C, Vázquez-Urbez M, Auqué L, Sancho C, Osácar C, Pardo G. 2014. Intrinsic and extrinsic controls of spatial and temporal variations in modern fluvial tufa sedimentation: A thirteen-year record from a semi-arid environment. *Sedimentology* 61: 90–132.

Arenas C, Piñuela L, García-Ramos JC. 2015. Climatic and tectonic controls on carbonate deposition in syn-rift siliciclastic fluvial systems: A case of microbialites and associated facies in the Late Jurassic. *Sedimentology* 62: 1149–1183.

Armienta MA, Vilaclara G, De la Cruz-Reyna S, Ramos S, Ceniceros N, Cruz O, *et al.* 2008. Water chemistry of lakes related to active and inactive Mexican volcanoes. *Journal of Volcanology and Geothermal Research* 178: 249–258.

Arp G. 1995. Lacustrine bioherms, spring mounds, and marginal carbonates of the Ries-Impact-Crater (Miocene, Southern Germany). *Facies* 33: 35–90.

Arp G, Reimer A, Reitner J. 1999. Calcification in cyanobacterial biofilms of alkaline salt lakes. *European Journal of Phycology* 34 (4): 393–403.

Ars J-M, Tarits P, Hautot S, Bellanger M, Coutant O, Maia M. 2019. Joint inversion of gravity and surface wave data constrained by magnetotelluric: Application to deep geothermal exploration of crustal fault zone in felsic basement. *Geothermics* 80: 56–68.

Aubert M, Bouiller R, Camus G, Cochet A, D'Arcy D, Giot D, *et al.* 1973. Notice de la carte géologique 1/50 000^{e}, Clermont-Ferrand. *BRGM* 63.

Awramik SM, Buchheim HP. 2012. The quest for microbialite analogs to the South Atlantic Pre-Salt carbonate hydrocarbon reservoirs of Africa and South America. *Houston Geol. Soc. Bull.* 55(1): 21, 23, 25, 27.

Baas-Becking LGM. 1925. Studies on the sulphur bacteria. *Annals of Botany* 39: 613–650.

Baumgartner LK, Reid RP, Dupraz C, Decho AW, Buckley DH, Spear JR, *et al.* 2006. Sulfate reducing bacteria in microbial mats: Changing paradigms, new discoveries. *Sed. Geol.* 185: 131–145.

Baumgartner LK, Spear JR, Buckley DH, Pace NR, Reid RP, Dupraz C, *et al.* 2009. Microbial diversity in modern marine stromatolites, Highborne Cay, Bahamas. *Environ. Microbiol.* 11: 2710–2719.

Bergerat F. 1987. Paléo-champs de contrainte tertiaires dans la plate-forme européenne au front de l'orogène Alpin. *Bulletin de la Société Géologique de France* 3: 611–620.

Bertrand-Sarfati J, Freytet P, Plaziat JC. 1966. Les calcaires concretionnes de la limite oligocene-miocene des environs de Saint-Pourcain-sur-Sioule (Limagne d'Allier) ; role des algues dans leur edification, analogie avec les stromatolites et rapports avec la sedimentation. *Bulletin de la Société Géologique de France* S7-VIII: 652–662.

Blair TC, McPherson JG. 2008. Quaternary sedimentology of the Rose Creek fan delta, Walker Lake, Nevada, USA, and implications to fan-delta facies models. *Sedimentology* 55: 579–615.

Bohacs KM, Carroll AR, Neal JE, Mankiewicz PJ. 2000. Lake-basin type, source potential, and hydrocarbon character: an integrated sequence-stratigraphic-geochemical framework. In: *Lake basins through space and time*. AAPG Studies in Geology 46: 3–34.

Bohacs KM, Lamb-Wozniak K, Demko TM, Eleson J, McLaughlin O, Lash C, *et al.* 2013. Vertical and lateral distribution of lacustrine carbonate lithofacies at the parasequence scale in the Miocene Hot Spring limestone, Idaho: An analog addressing reservoir presence and quality. *AAPG Bulletin* 97: 1967–1995.

Boomer SM, Noll KL, Geesey GG, Dutton BE. 2009. Formation of multilayered photosynthetic biofilms in an alkaline thermal spring in yellowstone national park, Wyoming. *Applied and Environmental Microbiology* 75: 2464–2475.

Bougeault C, Vennin E, Durlet C, Muller E, Mercuzot M, Chavez M, *et al.* 2019. Biotic–abiotic influences on modern Ca–Si-rich hydrothermal spring mounds of the pastos grandes volcanic Caldera (Bolivia). *Minerals* 9: 380.

Bouton A, Vennin E, Boulle J, Pace A, Bourillot R, Thomazo C, *et al.* 2016. Linking the distribution of microbial deposits from the Great Salt Lake (Utah, USA) to tectonic and climatic processes. *Biogeosciences Discuss* 2016: 1–26.

Bouton A, Vennin E, Amiotte-Suchet P, Thomazo C, Sizun J, Virgone A, *et al.* 2019. Prediction of the calcium carbonate budget in a sedimentary basin: A "source-to-sink" approach applied to Great Salt Lake, Utah, USA. *Basin Research*, 1–30.

Bradley WH. 1924. Fossil caddisfly cases from the Green River Formation of Wyoming. *American Journal of Science* 7: 310–312.

Brasier A, Wacey D, Rogerson M, Guagliardo P, Saunders M, Kellner S, *et al.* 2018. A microbial role in the construction of Mono Lake carbonate chimneys? *Geobiology* 16: 540–555.

Bräuer K, Kämpf H, Niedermann S, Wetzel H-U. 2017. Regional distribution pattern of carbon and helium isotopes from different volcanic fields in the French Massif Central: Evidence for active mantle degassing and water transport. *Chemical Geology* 469: 4–18.

BRGM. 2006. Carte géologique de France à 1/1 000 000, Clermont-Ferrand. *BRGM*.

Brock TD, Brock ML. 1971. Microbiological studies of thermal habitats of the central volcanic region, North Island, New Zealand. *New Zealand Journal of Marine and Freshwater Research* 5: 233–258.

Carozzi AV. 1962. Observations on Algal Biostromes in the Great Salt Lake, Utah. *The Journal of Geology* 70: 246–252.

Carroll AR, Bohacs KM. 1999. Stratigraphic classification of ancient lakes: Balancing tectonic and climatic controls. *Geology* 27: 99–102.

Casanova J. 1994. Stromatolites from the East African Rift: A synopsis. In: Bertrand-Sarfati J, Monty C, eds. *Phanerozoic Stromatolites II*. Dordrecht: Springer Netherlands, pp. 193–226.

Casanova J, Hillaire-Marcel C. 1992. Late holocene hydrological history of Lake Tanganyika, East Africa, from isotopic data on fossil stromatolites. *Palaeogeogr. Palaeoclimat. Palaeoecol.* 91: 35–48.

Casanova J, Bodenan F, Negrel P, Azaroual M. 1999. Microbial control on the precipitation of modern ferrihydrite and carbonate deposits from the Cézallier hydrothermal springs (Massif Central, France). *Sed. Geol.* 126: 125–145.

Castenholz RW. 1977. The effect of sulfide on the blue-green algae of hot springs II. Yellowstone National Park. *Microb Eco* 3: 79–105.

Ceraldi TS, Green D. 2017. Evolution of the South Atlantic lacustrine deposits in response to Early Cretaceous rifting, subsidence and lake hydrology. *Geological Society, London, Special Publications* 438: 77–98.

Cerling TE. 1994. Chemistry of closed basin lake waters: a comparison between African Rift Valley and some central North American rivers and lakes. In: Gierlowski-Kordesch EH, Kelts K, eds. *The Global Geological Record of Lake Basins*. Cambridge: Cambridge University Press, pp. 29–30.

Chafetz HS, Folk RL. 1984. Travertines; depositional morphology and the bacterially constructed constituents. *Journal of Sedimentary Research* 54: 289–316.

Chafetz HS, Guidry SA. 1999. Bacterial shrubs, crystal shrubs, and ray-crystal shrubs: bacterial vs. abiotic precipitation. *Sedimentary Geology* 126: 57–74.

Chafetz H, Barth J, Cook M, Guo X, Zhou J. 2018. Origins of carbonate spherulites: Implications for Brazilian Aptian pre-salt reservoir. *Sedimentary Geology* 365: 21–33.

Chateauneuf JJ. 1972. Contribution à l'étude de l'Aquitanien. La coupe de Carry-le-Rouet (Bouches-du-Rhône, France). V^{e} Congrès du Néogène méditerranéen. Volume III, Étude palynologique. *Bulletin Bureau de Recherches Géologiques et Minières* 4: 59–65.

Chazot G, Mergoil-Daniel J. 2012. Co-eruption of carbonate and silicate magmas during volcanism in the Limagne graben (French Massif Central). *Lithos* 154: 130–146.

Chidsey TC, Vanden Berg MD, Eby DE. 2015. Petrography and characterization of microbial carbonates and associated facies from modern Great Salt Lake and Uinta Basin's Eocene Green River Formation in Utah, USA. *Geological Society, London, Special Publications* 418: 261–286.

Christ N, Maerz S, Kutschera E, Kwiecien O, Mutti M. 2018. Palaeoenvironmental and diagenetic reconstruction of a closed-lacustrine carbonate system – The challenging marginal setting of the Miocene Ries Crater Lake (Germany). *Sedimentology* 65: 235–262.

Cohen AS, Talbot MR, Awramik SM, Dettman DL, Abell P. 1997. Lake level and paleoenvironmental history of Lake Tanganyika, Africa, as inferred from late Holocene and modern stromatolites. *Geol. Soc. Am. Bull.* 109: 444–460.

Coussement C, Gente P, Rolet J, Tiercelin JJ, Wafula M, Buku S. 1994. The North Tanganyika hydrothermal fields, East African Rift system: Their tectonic control and relationship to volcanism and rift segmentation. *Tectonophysics* 237: 155–173.

Crossey LJ, Karlstrom KE, Springer AE, Newell D, Hilton DR, Fischer T. 2009. Degassing of mantle-derived CO_2 and He from springs in the southern Colorado Plateau region – Neotectonic connections and implications for groundwater systems. *GSA Bulletin* 121: 1034–1053.

Cukur D, Krastel S, Cağatay MN, Damcı E, Meydan AF, Kim S-P. 2015. Evidence of extensive carbonate mounds and sublacustrine channels in shallow waters of Lake Van, eastern Turkey, based on high-resolution chirp subbottom profiler and multibeam echosounder data. *Geo-Mar. Lett.* 35: 329–340.

D'Halloy JJ. 1812. Sur le gisement du calcaire d'eau douce dans les départements du Cher, de l'Allier et de la Nièvre. *Journal des mines* 32: 43–64.

Dangeard L. 1931. Algues inférieures dans le calcaire concrétionné de la Limagne. *Compte Rendus Académie des Sciences Paris* 192: 172–174.

Davison I. 2007. Geology and tectonics of the South Atlantic Brazilian salt basins. *Geological Society, London, Special Publications* 272: 345–359.

De Boever E, Brasier AT, Foubert A, Kele S. 2017. What do we really know about early diagenesis of non-marine carbonates? *Sedimentary Geology* 361: 25–51.

De Lary L, Loschetter A, Gal F, Vanoudheusden E, Rocher P, Burnol A, *et al.* 2016. Risques liés aux émissions naturelles de CO_2 dans l'agglomération de Clermont-Ferrand. In: *Envirorisk forum*.

De Wet CB, Godfrey L, De Wet AP. 2015. Sedimentology and stable isotopes from a lacustrine-to-palustrine limestone deposited in an arid setting, climatic and tectonic factors: Miocene–Pliocene Opache Formation, Atacama Desert, Chile. *Palaeogeography, Palaeoclimatology, Palaeoecology* 426: 46–67.

Della Porta G. 2015. Carbonate build-ups in lacustrine, hydrothermal and fluvial settings: comparing depositional geometry, fabric types and geochemical signature. *Geological Society, London, Special Publications* 418: 17–68.

Dèzes P, Schmid SM, Ziegler PA. 2004. Evolution of the European Cenozoic Rift System: interaction of the Alpine and Pyrenean orogens with their foreland lithosphere. *Tectonophysics* 389: 1–33.

Donsimoni M. 1975. Étude des calcaires concrétionnés lacustres de l'Oligocène supérieur et de l'Aquitanien du bassin de Limagne (Massif Central, France). Thèse de 3^{e} cycle, Paris VI, 197 p.

Donsimoni M, Giot D. 1977. Les calcaires concrétionnés lacustres de l'Oligocène supérieur et de l'Aquitanien de Limagne (Massif central). *Bulletin du BRGM* 2: 131–169.

Dromart G, Gaillard C, Jansa LF. 1994. Deep-marine microbial structures in the Upper Jurassic of Western Tethys. In: Bertrand-Sarfati J, Monty C, eds. *Phanerozoic Stromatolites II*. Dordrecht: Springer Netherlands, pp. 295–318.

Dunagan SP, Driese SG. 1999. Control of terrestrial stabilization on Late Devonian palustrine carbonate deposition; Catskill Magnafacies, New York, USA. *Journal of Sedimentary Research* 69: 772–783.

Dupraz C, Visscher PT. 2005. Microbial lithification in marine stromatolites and hypersaline mats. *Trends Microbiol* 13: 429–38.

Dupraz C, Reid RP, Braissant O, Decho AW, Norman RS, Visscher PT. 2009. Processes of carbonate precipitation in modern microbial mats. *Earth-Science Reviews* 96: 141–162.

Dupraz C, Reid RP, Visscher P. 2011. Microbialites, modern. In: Reitner J, Thiel V, eds. *Encyclopedia of Geobiology*. Encyclopedia of Earth Sciences Series. Dordrecht, The Netherlands: Springer Netherlands, University of Göttingen, pp. 617–635.

Dupraz C, Fowler A. Tobias C, Visscher PT. 2013. Stromatolitic knobs in Storr's Lake (San Salvador, Bahamas): A model system for formation and alteration of laminae. *Geobiology* 11: 527–548.

Duwiquet H, Arbaret L, Guillou-Frottier L, Heap MJ, Bellanger M. 2019. On the geothermal potential of crustal fault zones: a case study from the Pontgibaud area (French Massif Central, France). *Geothermal Energy* 7: 33.

Eardley AJ. 1938. Sediments of Great Salt Lake, Utah. *AAPG Bulletin* 22: 1305–1411.

Farias F, Szatmari P, Bahniuk A, França AB. 2019. Evaporitic carbonates in the pre-salt of Santos Basin – Genesis and tectonic implications. *Marine and Petroleum Geology* 105: 251–272.

Fedorchuk ND, Dornbos SQ, Corsetti FA, Isbell JL, Petryshyn VA, Bowles JA, *et al.* 2016. Early non-marine life: Evaluating the biogenicity of Mesoproterozoic fluvial-lacustrine stromatolites. *Precambrian Research* 275: 105–118.

Flügel E. 2004. Microfacies of carbonate rocks: Analysis interpretation and application. Berlin: Springer, 976 p.

Folk RL. 1999. Nannobacteria and the precipitation of carbonate in unusual environments. *Sediment. Geol.* 126: 47–55.

Fouke BW. 2011. Hot-spring systems geobiology: Abiotic and biotic influences on travertine formation at Mammoth Hot Springs, Yellowstone National Park, USA. *Sedimentology* 58: 170–219.

Fouke BW, Farmer JD, Des Marais DJ, Pratt L, Sturchio NC, Burns RW, *et al.* 2000. Depositional facies and aqueous-solid geochemuistry and travertine-depositing hot springs (Angel Terrace, Mammoth Hot Springs, Yellowstone National Park, USA). *J. Sed. Res.* A70: 565–585.

Freytet P. 1998. Non-marine, Permian to Holocene algae from France and adjacent countries. *Annales de Paléontologie* 84: 3–51.

Freytet P. 2000. Distribution and palaeoecology of non marine algae and stromatolites: II, the limagne of allier Oligo-Miocene lake (central France). *Annales de Paléontologie* 86: 3–57.

Freytet P, Plet A. 1996. Modern freshwater microbial carbonates: the Phormidium stromatolites (tufa-travertine) of southeastern Burgundy (Paris Basin, France). *Facies* 34: 219–238.

Freytet P, Verrecchia EP. 1998. Freshwater organisms that build stromatolites: a synopsis of biocrystallization by prokaryotic and eukaryotic algae. *Sedimentology* 45: 535–563.

Gal F, Brach M, Braibant G, Bény C, Michel K. 2012. What can be learned from natural analogue studies in view of CO2 leakage issues in carbon capture and storage applications? Geochemical case study of Sainte-Marguerite area (French Massif Central). *International Journal of Greenhouse Gas Control* 10: 470–485.

Galloway W. 1975. Process framework for describing the morphologic and stratigraphic evolution of deltaic depositional system. *Society of Economic Paleontologists and Mineralogist (SEPM), Special Publication* 31: 127–156.

Garrett P. 1970. Phanerozoic stromatolites: Noncompetitive ecologic restriction by grazing and burrowing animals. *Science* 169: 171–173.

Genter A, Giot D, Lieutenant N, Nehlig P, Rocher P, Roig J-Y, *et al.* 2003. Méthodologie de l'inventaire géothermique des Limagnes : projet COPGEN. Compilation des données. BRGM/RP-52644-FR. Orléans, France : BRGM.

Ginsburg RN. 1991. Controversies about stromatolites: Vices and virtues. In: Müller DW, McKenzie JA, Weissert H, eds. *Controversies in Modern Geology*. London, UK: Academic Press, pp. 25–36.

Ginsburg RN, Planavsky NJ. 2008. Diversity of Bahamian microbialite substrates. In: Dilek Y, Furnes H, Muehlenbachs K, eds. *Links between Geological Processes, Microbial Activities & Evolution of Life*, 4. Dordrecht: Springer Netherlands, pp. 177–195.

Giot D, Gentilhomme P, Bouiller R, Clozier L, Fleury R, Gagnière G, *et al.* 1976. Notice de la carte géologique 1/50 000^{e}, Saint Pourçain sur Sioule. *BRGM* 16.

Goër de Hervé A. 2000. Peperites from the Limagne Trench (Auvergne, French Massif Central): A distinctive facies of phreatomagmatic pyroclastic. History of a semantic drift. In: Leyrit H, Montenant C, eds. *Volcaniclastic Rocks from Magmas to Sediments*. Amsterdam: Gordon and Breach Science Publishers, pp. 91–110.

Gomes JP, Bunevich RB, Tedeschi LR, Tucker ME, Whitaker FF. 2020. Facies classification and patterns of lacustrine carbonate deposition of the Barra Velha Formation, Santos Basin, Brazilian Pre-salt. *Marine and Petroleum Geology* 113: 104176.

Gong E, Xu J, Wang T, Liang Y, Gao F. 2017. Microbial–caddisfly bioherms in the Early Cretaceous Yixian Formation in the Yixian Basin, Western Liaoning, China. *Cretaceous Research* 78: 127–138.

Gorin G. 1975. Étude palynostratigraphique des sédiments paléogènes de la Grande Limagne (Massif central, France) : avec applications de la statistique et de l'informatique. *Bulletin du BRGM*, 147–181.

Gradziński M. 2010. Factors controlling growth of modern tufa: Results of a field experiment. *Geological Society, London, Special Publications* 336: 143–191.

Grolier J, Tchimichkian G. 1963. Connaissances nouvelles sur la geologie du socle de la Limagne d'apres les sondages de la Regie autonome des petroles. *Bulletin de la Société Géologique de France* S7-V: 930–937.

Guo X, Chafetz HS. 2012. Large tufa mounds, Searles Lake, California. *Sedimentology* 59: 1509–1535.

He X, Chen Z-Q, Lu Z, Li J, Hu W, Li S, Xu Z. 2015. Exceptionally preserved caddisfly larval cases (Insecta) from the lower Cretaceous of the Liupanshan basin, Western China. *Journal of Earth Science* 26: 192–202.

Herlinger R Jr, Zambonato EE, De Ros LF. 2017. Influence of diagenesis on the quality of Lower Cretaceous pre-salt lacustrine carbonate reservoirs from Northern Campos Basin, Offshore Brazil. *Journal of Sedimentary Research* 87: 1285–1313.

Hines ME, Visscher PT, Teske AP, Devereux R. 2007. Sulfur cycling. In: Hurst CJ, Crawford RL, Garland JL, Lipson DA, Mills AL, Stetzenbach LD, eds. *Manual of Environmental Microbiology*. Washington DC: ASM Press, pp. 618–639.

Hugueney M. 1984. Évolution du paléoenvironnement dans le tertiaire de Limagne (Massif Central, France) à partir des faunes de mammifères. *Geobios* 17: 385–391.

Hugueney M. 1997. Biochronologie mammalienne dans le Paléogène et le Miocène inférieur du Centre de la France : synthèse réactualisée. In: Aguilar J-P, Legendre S, Michaux J, eds. *Actes du Congrès BiochroM'97, 21*. Mémoires et Travaux de l'Institut de Montpellier de l'École Pratique des Hautes Études, Montpellier, pp. 417–430.

Hugueney M, Tachet H, Escuillié F. 1990. Caddisfly pupae from the Miocene indusial limestone of Saint-Gérand-le-Puy, France. *Paleontology* 33: 495–502.

Hugueney M, Poidevin J-L, Bodergat A-M, Caron J-B, Guérin C. 1999. Des mammifères de l'Aquitanien inférieur à La Roche-Blanche-Gergovie (Puy-de-Dôme, France), révélateurs de l'activité post-oligocène du rift en Limagne de Clermont. *Comptes Rendus de l'Académie des Sciences – Series IIA – Earth and Planetary Science* 328: 847–852.

Hugueney M, Berthet D, Bodergat A-M, Escuillié F, Mourer-Chauviré C, Wattinne A. 2003. La limite Oligocène-Miocène en Limagne : changements fauniques chez les mammifères, oiseaux et ostracodes des différents niveaux de Billy-Créchy (Allier, France). *Geobios* 36: 719–731.

Hurst P, Judge S, Werthmann E, Sheban M, Luna E, Reynolds R. 2018. An analysis of caddisfly larval cases from domal bioherms in the Upper Green River formation, White Hill Cuesta, Ephraim, Utah. In: *AAPG ACE*. AAPG Datapages.

Hutchinson MF. 1988. Calculation of hydrologically sound digital elevation models. In: *Proceedings of the Third International Symposium on Spatial Data Handling*, 133, International Geographical Union Sydney.

Hutchinson MF. 1989. A new procedure for gridding elevation and stream line data with automatic removal of spurious pits. *Journal of Hydrology* 106: 211–232.

Hyžný M, Šimo V, Starek D. 2015. Ghost shrimps (Decapoda: Axiidea: Callianassidae) as producers of an Upper Miocene trace fossil association from sublittoral deposits of Lake Pannon (Vienna Basin, Slovakia). *Palaeogeography, Palaeoclimatology, Palaeoecology* 425: 50–66.

Janecke SU, Evans JP. 2016. The Great Salt Lake fault and its microbial mounds. In: *Presentations for the annual Utah Fault Parameters Working Group (UQFPWG), Feb 10, 2016*, pp. 239–274. Available from http://files.geology.utah.gov/ghp/workgroups/pdf/uqfpwg/UQFPWG-2016_Presentations.pdf.

Janecke SU, Evans JP. 2017. Revised structure and correlation of the East Great Salt Lake, North Promontory, Rozel and Hansel Valley fault zones revealed by the 2015–2016 low stand of Great Salt Lake. In: Lund WL, Emerman SH, Wang W, Zanazzi A, eds. *Geology and Resources of the Wasatch: Back to Front*. Utah Geol. Assoc. Publ., Vol. 46, pp. 295–360.

Javor BJ, Castenholz RW. 1984. Productivity studies of microbial mats, Laguna Guerrero Negro, Mexico. In: Cohen Y, Castenholz RW, Halvorsen HO, eds. *Microbial Mats-Stromatolites*. New York: Allan R. Liss, pp. 149–170.

Jones WJ, Stugard CE, Jannasch HW. 1989. Comparison of thermophilic methanogens from submarine hydrothermal vents. *Arch. Microbiol.* 151: 314–319.

Kano A, Matsuoka J, Kojo T, Fujii H. 2003. Origin of annual laminations in tufa deposits, southwest Japan. *Palaeogeography, Palaeoclimatology, Palaeoecology* 191: 243–262.

Kempe S, Kazmierczak J, Landmann G, Konuk T, Reimer A, Lipp A. 1991. Largest known microbialites discovered in Lake Van. *Nature* 349: 605–608.

Koinig KA, Shotyk W, Lotter AF, Ohlendorf C, Sturm M. 2003. 9000 years of geochemical evolution of lithogenic major and trace elements in the sediment of an alpine lake–the role of climate, vegetation, and land-use history. *Journal of Paleolimnology* 30: 307–320.

Kreuser T. 1995. Tectonic and climatic controls of lacustrine sedimentation in pre-rift and rift settings in the Permian-Triassic of East Africa. *Journal of Paleolimnology* 13: 3–19.

Lang J. 1984. Un environnement carbonaté palustro-lacustre et hydrothermal : le barrage quaternaire du Dragon (Bassin de Bamyan – Afghanistan Central). *Geobios* 17: 251–260.

Lee H, Muirhead JD, Fischer TP, Ebinger CJ, Kattenhorn SA, Sharp ZD, *et al.* 2016. Massive and prolonged deep carbon emissions associated with continental rifting. *Nature Geoscience* 9: 145–149.

Leggitt VL, Cushman RA. 2001. Complex caddisfly-dominated bioherms from the Eocene Green River Formation. *Sedimentary Geology* 145: 377–396.

Leggitt VL, Biaggi RE, Buchheim HP. 2007. Palaeoenvironments associated with caddisfly-dominated microbial-carbonate mounds from the Tipton Shale Member of the Green River Formation: Eocene Lake Gosiute. *Sedimentology* 54: 661–699.

Lima BEM, De Ros LF. 2019. Deposition, diagenetic and hydrothermal processes in the Aptian Pre-Salt lacustrine carbonate reservoirs of the northern Campos Basin, offshore Brazil. *Sedimentary Geology* 383: 55–81.

Loewen MA, Leggitt VL, Buchheim HP. 1999. Caddisfly (Trichoptera) larval cases from Eocene Fossil Lake, Fossil Butte National Monument. NPS/NRGRD/GRDTR-99/03, National Park Service Paleontological Research, United States Department of the Interior National Parks Service, Geological Resource Division Lakewood, CO, USA.

Mackay RJ, Wiggins GB. 1979. Ecological diversity in Trichoptera. *Annual Review of Entomology* 24: 185–208.

Madsen DB, Rhode D, Grayson DK, Broughton JM, Livingston SD, Hunt J, *et al.* 2001. Late Quaternary environmental change in the Bonneville basin, Western USA. *Palaeogeography, Palaeoclimatology, Palaeoecology* 167: 243–271.

Mallard E. 1890. Sur la lussatite, nouvelle variété minérale cristallisée de silice. *Bulletin de Minéralogie* 13: 63–66.

Manzo E, Perri E, Tucker ME. 2012. Carbonate deposition in a fluvial tufa system: processes and products (Corvino Valley-southern Italy): Carbonate fluvial tufa deposition, processes and products. *Sedimentology* 59: 553–577.

Megonigal JP, Hines ME, Visscher PT. 2003. Anaerobic metabolism and production of trace gases. In: Holland HD, Turekian KK, eds. *Treatise on Geochemistry*, Vol. 8. Elsevier, pp. 317–424.

Mello MR, De Azambuja Filho NC, Bender AA, Barbanti SM, Mohriak W, Schmitt P, *et al.* 2013. The Namibian and Brazilian southern South Atlantic petroleum systems: are they comparable analogues? *Geological Society, London, Special Publications* 369: 249–266.

Merle O, Michon L. 2001. The formation of the West European Rift; a new model as exemplified by the Massif Central area. *Bulletin de la Société Géologique de France* 172(2): 213–221.

Merle O, Michon L, Camus G, de Goer A. 1998. L'extension oligocène sur la transversale septentrionale du rift du Massif Central. *Bulletin de la Société Géologique de France* 169: 615–626.

Merz-Preiß M, Riding R. 1999. Cyanobacterial tufa calcification in two freshwater streams: ambient environment, chemical thresholds and biological processes. *Sedimentary Geology* 126(1-4): 103–124

Michon L. 2000. Dynamique de l'extension continentale : application au Rift Ouest-Européen par l'étude de la province du Massif Central. PhD Thesis, Université Blaise Pascal, Clermont-Ferrand II, 266 p.

Michon L, Merle O. 2001. The evolution of the Massif Central Rift; spatio-temporal distribution of the volcanism. *Bulletin de la Société Géologique de France* 172: 201–211.

Middleton V, Coniglio M, Hardie LA, Longstaffe FJ. 2005. Encyclopedia of sediments and sedimentary rocks, pp. 928.

Morange A, Heritier F, Villemin J. 1971. Contribution de l'exploration pétrolière à la connaissance structurale et sédimentaire de la Limagne, dans le Massif Central. In: *Géologie, géomorphologie et structure profonde du Massif Central français*. Symp. J. Jung, Clermont-Ferrand, pp. 295–308.

Mtelela C, Roberts EM, Downie R, Hendrix MS. 2016. Interplay of structural, climatic, and volcanic controls on late quaternary lacustrine–deltaic sedimentation patterns in the Western Branch of the East African Rift System, Rukwa Rift Basin, Tanzania. *Journal of Sedimentary Research* 86: 1179–1207.

Muniz MC, Bosence DWJ. 2015. Pre-salt microbialites from the Campos Basin (offshore Brazil): image log facies, facies model and cyclicity in lacustrine carbonates. *Geological Society, London, Special Publications* 418: 221–242.

Olariu C, Bhattacharya JP. 2006. Terminal distributary channels and delta front architecture of river-dominated delta systems. *Journal of Sedimentary Research* 76: 212–233.

Owen RB, Crossley R. 1992. Spatial and temporal distribution of diatoms in sediments of lake Malawi, central Africa, and ecological implications. *Journal of Paleolimnology* 7: 55–71.

Pace A, Bourillot R, Bouton A, Vennin E, Galaup S, Bundeleva I, *et al.* 2016. Microbial and diagenetic steps leading to the mineralisation of Great Salt Lake microbialites. *Scientific Reports* 6: 31495.

Pace A, Bourillot R, Bouton A, Vennin E, Braissant O, Dupraz C, *et al.* 2018. Formation of stromatolite lamina at the interface of oxygenic-anoxygenic photosynthesis. *Geobiology* 16: 378–398.

Pache M, Reitner J, Arp G. 2001. Geochemical evidence for the formation of a large miocene "travertine" mound at a sublacustrine spring in a soda lake (Wallerstein castle rock, nördlinger ries, Germany). *Facies* 45: 211–230.

Paik IS. 2005. The oldest record of microbial-caddisfly bioherms from the Early Cretaceous Jinju Formation, Korea: occurrence and palaeoenvironmental implications. *Palaeogeography, Palaeoclimatology, Palaeoecology* 218: 301–315.

Payandi-Rolland D, Roche A, Vennin E, Visscher PT, Amiotte-Suchet P, Thomas C, *et al.* 2019. Carbonate precipitation in mixed cyanobacterial biofilms forming freshwater microbial tufa. *Minerals* 9(7): 409.

Pedley HM. 1990. Classification and environmental models of cool freshwater tufas. *Sed. Geol.* 68: 143–154.

Pedley M. 1992. Freshwater (phytoherm) reefs: the role of biofilms and their bearing on marine reef cementation. *Sed. Geol.* 79: 255–274.

Pedley M. 2014. The morphology and function of thrombolitic calcite precipitating biofilms: A universal model derived from freshwater mesocosm experiments. *Sedimentology* 61: 22–40.

Pelletier H. 1972. Notes géologiques sur la Limagnes. *Revue des sciences naturelles d'Auvergne* 38: 7–19.

Pentecost A. 2005. Travertine. Berlin: Springer-Verlag, 445 p.
Perri E, Manzo E, Tucker ME. 2012. Multi-scale study of the role of the biofilm in the formation of minerals and fabrics in calcareous tufa. *Sediment. Geol.* 263-264: 16–29.
Perrier G, Ruegg JC. 1973. Structure profonde du Massif Central français. *Ann. Geophys.* 29: 435–502.
Pettijohn FJ, Potter PE, Siever R. 2012. Sand and sandstone. Berlin: Springer-Verlag, 618 p.
Platt NH. 1989. Climatic and tectonic controls on sedimentation of a Mesozoic lacustrine sequence: The purbeck of the Western Cameros Basin, Northern Spain. *Palaeogeography, Palaeoclimatology, Palaeoecology* 70: 187–197.
Platt NH, Wright VP. 1991. Lacustrine carbonates: facies models, facies distributions and hydrocarbon aspects. In: Anadon P, Cabrera L, Kelts K, eds. *Lacustrine Facies Analysis*. Oxford, UK: Blackwell Publishing Ltd, pp. 57–74.
Reid RP, Visscher PT, Decho AW, Stolz JF, Bebout BM, Dupraz C, *et al.* 2000. The role of microbes in accretion, lamination and early lithification of modern marine stromatolites. *Nature* 406: 989–992.
Reis OM. 1921. Erläuterungen zu dem Blatte Donnersberg (Nr. XXI) der Geognostische Karte von Bayern: 1: 100 000. Piloty & Loehle, 320 p.
Renaut RW, Owen RB, Ego JK. 2017. Geothermal activity and hydrothermal mineral deposits at southern Lake Bogoria, Kenya Rift Valley: Impact of lake level changes. *Journal of African Earth Sciences* 129: 623–646.
Rey R. 1964. L'Oligocène et le Miocène inférieur de la Limagne Bourbonnaise. *Revue scientifique du Bourbonnais*, 56–81.
Rey R. 1971. Biostratigraphie des bassins tertiaires du Massif Central. In: *Géologie, géomorphologie et structure profonde du Massif Central*. Symp. J. Jung. Clermont-Ferrand, pp. 309–330.
Riding R. 1979. Origin and diagenesis of lacustrine algal bioherms at the margin of the Ries crater, Upper Miocene, southern Germany. *Sedimentology* 26: 645–680.
Riding R. 2008. Abiogenic, microbial and hybrid authigenic crusts: Components of Precambrian stromatolites. *Geologica Croatica* 61: 105–111.
Riding R. 2011. Microbialites, stromatolites, and thrombolites. In: *Encyclopedia of Geobiology.* Springer, pp. 635–654.
Riding R, Virgogne A. 2020. Hybrid Carbonates: in situ abiotic, microbial and skeletal co-precipitates. *Earth Sciences Review* 208: 1–23.
Rieger T. 1992. Calcareous tufa formations. Searles L*ake and Mono Lake: California Geology* 45: 99–109.
Rihs S, Condomines M, Poidevin J-L. 2000. Long-term behaviour of continental hydrothermal systems: U-series study of hydrothermal carbonates from the French Massif Central (Allier Valley). *Geochimica et Cosmochima Acta* 64: 3189–3199.
Riveline J, Giot D, Farjanel G, Pacquet A. 1988. Mise en évidence de dépôts Eocène moyen (Lutétien supérieur) à la base des formations Tertiaires du bassin de Moulins (Allier, France) : implications tectoniques. *Comptes rendus de l'Académie des sciences. Série 2, Mécanique, Physique, Chimie, Sciences de l'univers, Sciences de la Terre* 306: 55–62.
Roche A, Vennin E, Bouton A, Olivier N, Wattinne A, Bundeleva I, *et al.* 2018. Oligo-Miocene lacustrine microbial and metazoan buildups from the Limagne Basin (French Massif Central). *Palaeogeography, Palaeoclimatology, Palaeoecology* 504: 34–59.
Roche A, Vennin E, Bundeleva I, Bouton A, Payandi-Rolland D, Amiotte-Suchet P, *et al.* 2019. The role of the substrate on the mineralization potential of microbial mats in a modern freshwater river (Paris Basin, France). *Minerals* 9: 359.
Rodríguez-Berriguete Á, Alonso-Zarza AM. 2019. Controlling factors and implications for travertine and tufa deposition in a volcanic setting. *Sedimentary Geology* 381: 13–28.
Ronchi P, Cruciani F. 2015. Continental carbonates as a hydrocarbon reservoir, an analog case study from the travertine of Saturnia, Italy. *AAPG Bulletin* 99(4): 711–734.
Rosen MR, Arehart GB, Lico MS. 2004. Exceptionally fast growth rate of < 100-yr-old tufa, Big Soda Lake, Nevada: Implications for using tufa as a paleoclimate proxy. *Geology* 32(5): 409–412.
Rosenfeld WD. 1947. Anaerobic oxidation of hydrocarbons by sulfate-reducing bacteria. *Journal of Bacteriology* 54: 664–665.
Rowland JV, Sibson RH. 2004. Structural controls on hydrothermal flow in a segmented rift system, Taupo Volcanic Zone, New Zealand. *Geofluids* 4: 259–283.
Saint Martin JP, Saint Martin S. 2016. Calcareous microbialites and associated biota in the mediterranean coastal lagoons and ponds of southern france: a key for ancient bioconstructions? *Geo-Eco-Marina* 55.
Scherer CMS, Lavina ELC, Dias Filho DC, Oliveira FM, Bongiolo DE, Aguiar ES. 2007. Stratigraphy and facies architecture of the fluvial–aeolian–lacustrine Sergi Formation (Upper Jurassic), Recôncavo Basin, Brazil. *Sedimentary Geology* 194: 169–193.
Scherler L, Mennecart B, Hiard F, Becker D. 2013. Evolutionary history of hoofed mammals during the Oligocene–Miocene transition in Western Europe. *Swiss J. Geosci.* 106: 349–369.
Schlager W. 2000. Carbonate depositional systems – From factories to sequences. *Mitt. Ges. Geol. Bergbaustud. Österr* 43: 119–121.
Schlager W. 2003. Benthic carbonate factories of the Phanerozoic. *Int. J. Earth Sci. (Geol. Rundsch.)* 92: 445–464.
Schnurrenberger D, Russell J, Kelts K. 2003. Classification of lacustrine sediments based on sedimentary components. *Journal of Paleolimnology* 29: 141–154.
Schuster M, Nutz A. 2018. Lacustrine wave-dominated clastic shorelines: modern to ancient littoral landforms and deposits from the Lake Turkana Basin (East African Rift System, Kenya). *Journal of Paleolimnology* 59: 221–243.
Seard C, Camoin G, Rouchy J-M, Virgone A. 2013. Composition, structure and evolution of a lacustrine carbonate margin dominated by microbialites: Case study from the Green River formation (Eocene; Wyoming, USA). *Palaeogeography, Palaeoclimatology, Palaeoecology* 381-382: 128–144.
Serra H, Petelet-Giraud E, Négrel P. 2003. Inventaire du potentiel géothermique de la Limagne (COPGEN). Synthèse bibliographique de la géochimie des eaux thermales. In: *Rap. BRGM/RP-52587-FR*.
Shapiro RS. 2000. A comment on the systematic confusion on thrombolites. *Palaios* 15: 166–169.
Sissingh W. 2001. Tectonostratigraphy of the West Alpine Foreland: Correlation of tertiary sedimentary sequences, changes in eustatic sea-level and stress regimes. *Tectonophysics* 333: 361–400.
Skilling IP, White JDL, McPhie J. 2002. Peperite: A review of magma–sediment mingling. *Journal of Volcanology and Geothermal Research* 114: 1–17.
Sobolev SV, Zeyen H, Granet M, Achauer U, Bauer C, Werling F, *et al.* 1997. Upper mantle temperatures and lithosphere-asthenosphere system beneath the French Massif Central constrained by seismic, gravity, petrologic and thermal observations. *Tectonophysics* 275: 143–164.
Souza RS, Arienti LM, Viana SM, Falcão LC, Cuglieri MA, Silva Filho RP, *et al.* 2018. Petrology of the hydrothermal and evaporitic continental cretaceous (Aptian) pre-salt carbonates and associated rocks, South Atlantic Santos Basin, Offshore Brazil. In: *AAPG ACE 2018*.

Swirydczuk K, Wilkison BH, Smith GR. 1979. The Pliocene Glenns Ferry Oolite: Lake-margin Carbonate Deposition in the Southwestern Snake River Plain. *SEPM Journal of Sedimentary Research* 49.

Szatmari P, Milani EJ. 2016. Tectonic control of the oil-rich large igneous-carbonate-salt province of the South Atlantic rift. *Marine and Petroleum Geology* 77: 567–596.

Taylor MP, Drysdale RN, Carthew KD. 2004. The formation and environmental significance of calcite rafts in tropical tufa depositing rivers of northern Australia. *Sedimentology* 51: 1089–1101.

Teboul PA, Durlet C, Gaucher EC, Virgone A, Girard JP, Curie J, *et al.* 2016. Origins of elements building travertine and tufa: New perspectives provided by isotopic and geochemical tracers. *Sedimentary Geology* 334: 97–114.

Tinsley BE, Grubbs SA, Yates JM, Meier AJ. 2016. Notes on the ecological roles of Podostemum *ceratophyllum Michx*, 1803 and *Cladophora glomerata* (L.) Kütz, 1843 in the habitat and diet of riverine hydropsychid caddisflies (Trichoptera). *Aquatic Insects* 37: 225–239.

Tucker ME, Wright VP. 1990. Carbonate sedimentology. Oxford, UK: Blackwell Publishing Ltd.

Utescher T, Mosbrugger V, Ashraf AR. 2000. Terrestrial climate evolution in north-west Germany over the last 25 million years. *Palaios* 15: 430–449.

Vanden Berg MD. 2019. Domes, rings, ridges, and polygons: characteristics of microbialites from Utah's Great Salt Lake. *The Sedimentary Record* 17(1): 4–10.

Vasconcelos C, McKenzie JA. 1997. Microbial mediation of modern dolomite precipitation and diagenesis under anoxic conditions (Lagoa Vermelha, Rio de Janeiro, Brazil). *Journal of Sedimentary Research* 67: 378–390.

Vennin E, Bouton A, Bourillot R, Pace A, Roche A, Brayard A, *et al.* 2019. The lacustrine microbial carbonate factory of the successive Lake Bonneville and Great Salt Lake, Utah, USA. *Sedimentology* 66: 165–204.

Visscher PT, Stolz JF. 2005. Microbial mats as bioreactors: populations, processes, and products. *Palaeogeography, Palaeoclimatology, Palaeoecology* 219: 87–100.

Visscher PT, Beukema J, van Gemerden H. 1991. In situ characterization of sediments: Measurements ofoxygen and sulfide profiles with a novel combined needle electrode. *Limnology and Oceanography* 36: 1476–1480.

Visscher PT, Reid RP, Bebout BM, Hoeft SE, Macintyre IG, Thompson JA. 1998. Formation of lithified micritic laminae in modern marine stromatolites (Bahamas); the role of sulfur cycling. *American Mineralogist* 83: 1482–1493.

Visscher PT, Reid RP, Bebout BM. 2000. Microscale observations of sulfate reduction: Correlation of microbial activity with lithified micritic laminae in modern marine stromatolites. *Geology* 28: 919–922.

Wasson MS, Saller A, Andres M, Self D, Lomando A. 2012. Lacustrine microbial carbonate facies in core from the lower Cretaceous Toca Formation, Block 0, offshore Angola. In: *American Association of Petroleum Geologists, Hedberg Conference: Microbial Carbonate Reservoir Characterization*.

Wattinne A. 2004. Évolution d'un environnement carbonate lacustre à bioconstructions, en limagne bourbonnaise (Oligo-Miocène, Massif Central, France). Paris : Muséum national d'histoire naturelle, 195 p.

Wattinne A, Vennin E, De Wever P. 2003. Evolution d'un environnement carbonaté lacustre à stromatolithes, par l'approche paléo-écologique (carrière de Montaigu-le-Blin, bassin des Limagnes, Allier, France). *Bulletin de la Société Géologique de France* 174: 243–260.

Wattinne A, Lécuyer C, Vennin E, Chateauneuf JJ, Martineau F. 2018. Environmental changes around the Oligocene/Miocene boundary in the Limagne graben, Massif Central, France. *Bulletin de la Société Géologique de France,* 189, 1–19.

Wilks M, Kendall JM, Nowacki A, Biggs J, Wookey J, Birhanu Y, *et al.* 2017. Seismicity associated with magmatism, faulting and hydrothermal circulation at Aluto Volcano, Main Ethiopian Rift. *Journal of Volcanology and Geothermal Research* 340: 52–67.

Winsborough BM, Seeler JS, Golubic S, Folk RL, Maguire B. 1994. Recent fresh-water lacustrine stromatolites, stromatolitic mats and oncoids from Northeastern Mexico. In: Bertrand-Sarfati J, Monty C, eds. *Phanerozoic Stromatolites II*. Dordrecht: Springer Netherlands, pp. 71–100.

Wright VP. 2021. The mantle, CO_2 and the giant Aptian chemogenic lacustrine carbonate factory of the South Atlantic: Some carbonates are made, not born. *Sedimentology*. https://doi.org/10.1111/sed.12835.

Wright VP, Barnett AJ. 2015. An abiotic model for the development of textures in some South Atlantic early Cretaceous lacustrine carbonates. *Geological Society, London, Special Publications* 418: 209–219.

Yemane K, Siegenthaler C, Kelts K. 1989. Lacustrine environment during Lower Beaufort (Upper Permian) Karoo deposition in Northern Malawi. *Palaeogeography, Palaeoclimatology, Palaeoecology* 70: 165–178.

Zachos J. 2001. Trends, rhythms, and aberrations in global climate 65 Ma to present. *Science* 292: 686–693.

Zeyen H, Novak O, Landes M, Prodehl C, Driad L, Hirn A. 1997. Refraction-seismic investigations of the northern Massif Central (France). *Tectonophysics* 275: 99–117.

Zhu X, Li S, Wu D, Zhu S, Dong Y, Zhao D, *et al.* 2017. Sedimentary characteristics of shallow-water braided delta of the Jurassic, Junggar basin, Western China. *Journal of Petroleum Science and Engineering* 149: 591–602.

Cite this article as: Vennin E, Bouton A, Roche A, Gérard E, Bundeleva I, Boussagol P, Wattinne A, Kolodka C, Gaucher E, Virgone A, Visscher PT. 2021. The Limagne Basin: a journey through modern and fossil microbial deposits, *BSGF - Earth Sciences Bulletin* 192: 41.